Automation in Construction 138 (2022) 104198

Contents lists available at ScienceDirect

Automation in Construction

journal homepage: www.elsevier.com/locate/autcon

Parametric design and robotic fabrication of whole timber reciprocal structures

Julien Geno, Justin Goosse, Serena Van Nimwegen, Pierre Latteur *

Université catholique de Louvain, UCLouvain, Civil and Environmental Engineering, Place du Levant, 1 (Vinci), bte L5.05.01, 1348 Louvain-la-Neuve, Belgium

ARTICLE INFO

Keywords:
Whole timber
Round timber
Log
Trunk
Raw timber
Heavy timber
Tall timber
Parametric design
Reciprocal structures
Automation
Robotic arm
Robot

ABSTRACT

To decrease the impact of the construction sector on climate change, sufficiently economic processes must urgently be developed to encourage the use of minorly transformed timber, such as tree trunks. However, the question remains how to inexpensively incorporate tree trunks with irregular morphology into structural systems from design to fabrication. It is only within recent years that robotic tools and parametric design software have made it possible to both quickly and affordably build with elements of geometry as variable as tree trunks. The objective of this article is to describe an automatic process, from parametric design to robotic fabrication, that makes it possible to build a full-scale structure from reshaped tree trunks. This research brings to light the scientific and technical challenges that must be undertaken before industrialization can be realized, therefore the geometric parametrization required of trunk-to-trunk connections is detailed herein. Finally, the authors describe a case study from design to fabrication of a full-scale $10 \text{ m} \times 5 \text{ m}$ reciprocal structure prototype made from fourteen tree trunk elements fabricated as described above using robotic arms. It is seen that reciprocal structures can span large distances with logs of limited length, but their structural complexity brings additional challenges to the design and construction processes. This study highlights not only the need for future development to accelerate the processes of automatic scanning and cutting of timber logs, but also for mechanical characterization of logs using non-destructive methods and better prediction of transmission of stresses in wood-wood assemblies.

1. Introduction

The following definitions are used in this article:

- “Whole timber” or “Unsawn wood” or “Log” or “Trunk”: a piece of tree trunk without branches and which has not been cut into smaller pieces.
- “Engineered timber”: used for all altered wood products e.g.: glue laminated timber or cross laminated timber.
- “Joint” or “connection”: refers to the place where two tree trunks meet, one being supported and the other being load-bearing. A joint or connection consists of two notches.
- “Notch”: at the place of a connection, it is the volume of wood that has been removed when machining a trunk.
- “Machining”: the process of mechanically removing a volume of a workpiece.
- “Cut”, or “cutting”: a basic notch that can be made in one step with a cutter that acts perpendicular to a main surface of the cut. A joint/connection is thus composed of 2 notches (one on each trunk), and a notch is composed of several cuts.
- “CNC”: “Computer Numerical Control”, which means a computer-controlled machine tool.
- “JJP connection”: name given by the authors to the connection they describe in this article, and which is detailed in sections 3.4 and 3.5.

1.1. The relevance of building with trunks

The increase in environmental awareness over the past two decades is prompting a re-evaluation of the way natural resources are used. This has an impact on the construction sector, which is not only one of the largest producers of waste in the EU [1], but also one of the main contributors to greenhouse gas emissions worldwide [2]. In this context,

* Corresponding author.
E-mail addresses: julien.geno@uclouvain.be (J. Geno), justin.goosse@uclouvain.be (J. Goosse), serena.vannimwegen@uclouvain.be (S. Van Nimwegen), pierre.latteur@uclouvain.be (P. Latteur).

https://doi.org/10.1016/j.autcon.2022.104198
Received 4 August 2021; Received in revised form 29 January 2022; Accepted 2 March 2022
Available online 11 April 2022

timber, as a renewable resource, is a material to be preferred in this sector. In fact, (i) the transformation of wood into construction products is one of the lowest producers of CO_2 across construction materials, (ii) building with timber stores CO_2 rather than releasing it into the atmosphere and (iii) there is potential for low emission recycling at the end of the building lifecycle. The condition for a sustainable approach is obviously twofold: in the one hand, systematic replanting of forests and good management according to labels such as PEFC (Programme for the Endorsement of Forest Certification), and diversified plantations to enhance biodiversity on the other hand. However, most major timber projects today are designed with beams, columns, or panels made with rectangular sections cut from trees with inherently great natural strength for response to extreme lateral loads like storms. The transformation steps required to make timber products creates (i) waste material by extracting a rectangular section beam from a conical tree trunk, (ii) a decrease in the mechanical characteristics due to broken fiber continuity around knots [3], (iii) an increased CO_2 impact, and (iv) high production costs due to all required operations. For example, the industrial production process of engineered timber starts with the sawing of the log where a large amount of material is lost. This is followed by drying, jointing, planing, pressing, and sanding. These steps increase the price of timber, which often decreases attractiveness compared to other building materials, thus discouraging use. Considering the aforementioned, it can be concluded that building structures with raw tree trunks is sensible, and researchers increasingly agree, as shown by the state of the art [3].

A major problem of timber construction is the long drying time of timber; often two years or more are necessary for trunks to obtain balance with air moisture content at the construction location. Therefore, two possibilities are available: (i) either logs are dried in a kiln, which is more expensive and less sustainable, or (ii) green timber logs are used. When using green logs, structures and connections must then be designed with tolerances to accommodate significant dimensional variations and the development of cracks. In this case, a longitudinal slit can be made on the trunk with a maximum of depth of between 30 and 50% of the diameter [4], which will not reduce dimensional variations, but it does reduce uncontrolled cracks. Furthermore, before reaching a low-cost industrial process, some scientific and technical challenges exist, including:

- The development of equipment and protocols that allow the mechanical characterization of trunks in order to predict their bearing capacity.
- The development of tools capable of a fast 3D scanning of trunks.
- The development of parametric design tools capable of shaping connections between trunks and sending comprehensible data to the machining tools.
- Research to evaluate how stresses are distributed in the connection interface between trunks, despite variations in moisture and overall deformation of the structure.
- Cheap structures and connections that allow large spans from trunks of limited length.
- And finally, a selection of the most efficient trunk-to-trunk connections suitable for both industrial cutting with robots and parametric design, with as little steel as possible. Stacked wooden cottages are an interesting source of inspiration, as shown in Fig. 1 [5]. However, most of these structures are built with calibrated logs and not raw logs. Cutting is done mostly on site and by hand, which requires skilled carpenters.

The objective of this article is to demonstrate the feasibility of a design and construction processes for structures made of tree trunks based on a framework of automatic cutting of adequately selected connections by a robotic arm that receives fabrication instructions from parametric design software. Specifically, reciprocal structures give meaning to this approach as they allow large spans with limited trunk lengths. Moreover, the connections are all different, which further justifies the relevance of robots for cutting when considering cost and timeliness. Nevertheless, the approach developed here is compatible with simple structures such as trunk frames or structures with stacked timber.

This article does not concern the mechanical characterization of logs (Regarding this, please refer to section 2.4: State of the art, Mechanical characterization of logs), the transmission of stresses in the connections, the influence of the connections' behavior on the global behavior of the structure, which are topics largely lacking in the state of the art. These require extensive research which exceeds the scope of this article.

1.2. Highlighting the limits of typical machining tools

Fig. 1 adequately illustrates the type of cuts that a log-log connection requires. The connection that has been selected has several cutting planes and is explained in depth in sections 3.4 and 3.5. Fig. 2 provides an overview, while Fig. 21 provides a diagram of the connection.

There are two opposite ways to sculpt objects with machining tools:

- The reference is placed on the tool itself, for instance one or several planes or points in relation to which the work piece is placed. This is what is usually done when using a CNC.
- The reference can be placed on the object itself if the work piece is an object with rough geometry, such as a tree trunk.

Sculpting a notch with typical machining, before the programming sophisticated robots, provides useful information about:

- The limitations of typical tools such as CNC tools.
- The relevance and the challenges inherent to the use of robotic arms.
- The advantages in time and precision that robotic arms can provide.
- The ways to design the most simplified connections possible.

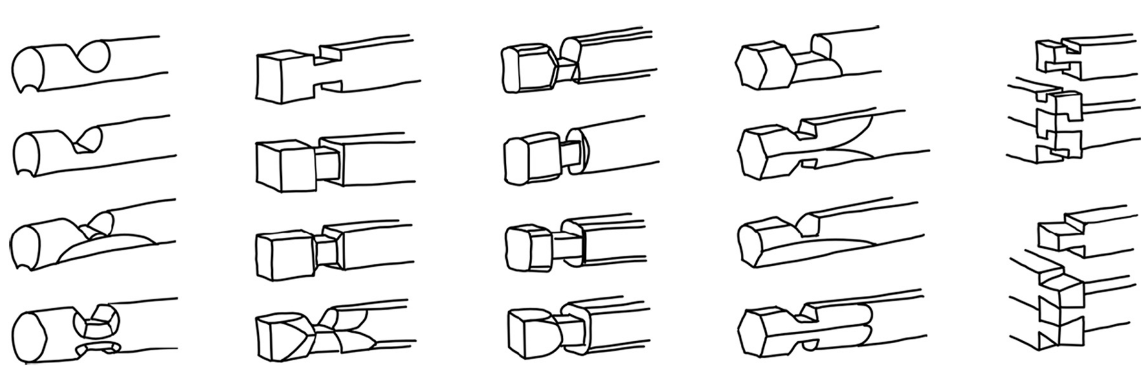

Fig. 1. Different types of joints for timber stacked with calibrated logs inspired from the book of Gerda Boëthius published in 1927 [5].

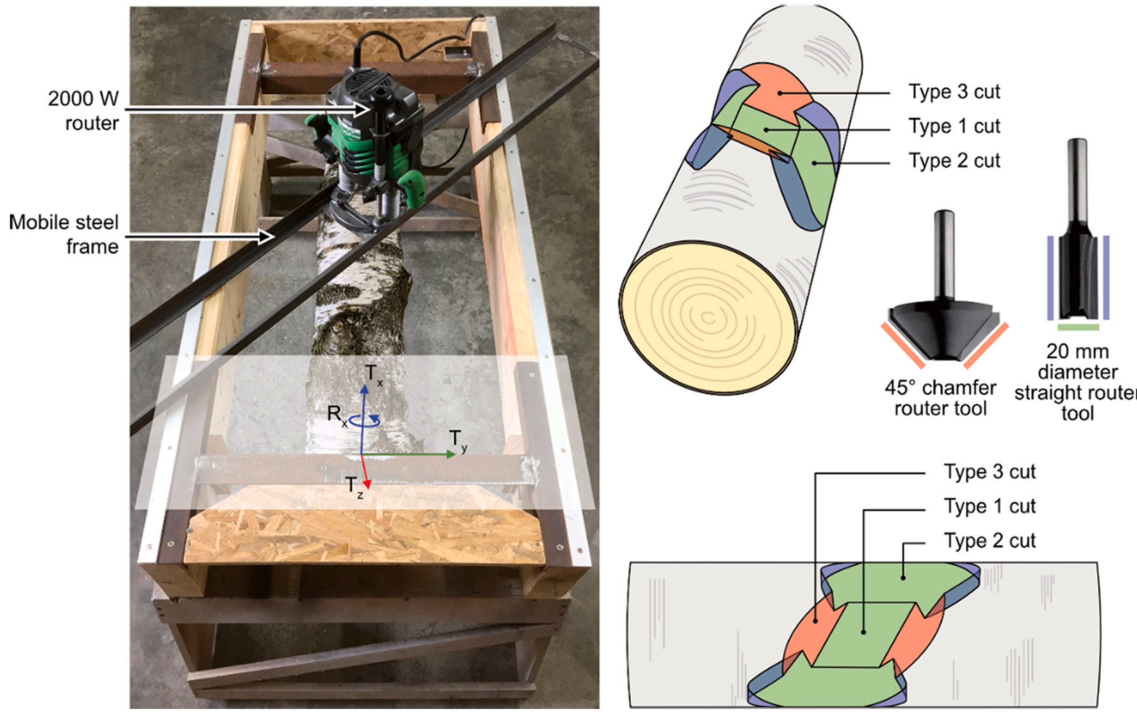

Fig. 2. "Homemade" machining bench.

This "homemade" machining bench (Fig. 2) consists of a fixed frame inside which the log is placed. The router is set on a mobile steel frame which can be moved in the X-Y horizontal plane. The log is supported at both ends and a rotation according to the X-axis (trunk axis) is possible. There are thus four degrees of freedom to perform the machining: three in translation (although the depth, Z, is limited at 65 mm by the range of the router), and one in rotation. A 45° chamfer tool and a 20 mm diameter straight tool are alternately fixed on the router to complete the machining equipment and increase the cutting functionality. Just like for a standard 3-axis CNC, the reference is in the horizontal X-Y plane in relation to which the work piece must be placed correctly but in a different orientation for each cut to be made.

There are three work piece sculpting processes for making cuts:

- Step 1, Making type 2 cuts (shown in Fig. 3): The contour of these cuts is defined by the interface between the numerical model of the work piece and the piece with which it must fit as a pair (contour = outline of the type 2 cut-out). The 3D models of each work piece and the contour was obtained with photogrammetry. Augmented reality was used to materialize this contour on the workpiece. Using the Fologram [6] plugin of the Grasshopper software, a smartphone was used to superimpose on the real work piece its own digital image and the image of the contour on the smartphone screen. This made it possible to mark the contour by hand directly on the work piece at the same time. The area was then hollowed out with the straight router tool, taking care to stay in the contour.
- Step 2, Making type 1 cuts (shown in Fig. 4): The router is free to move in the X and Y directions into an area limited by two aluminum bars spaced such that the width of the base end-cut is respected (straight lines A-A and B-B in the plane X-Y).
- Step 3, Making type 3 cuts (shown in Fig. 5): This process is similar to the process related to type 1 cuts, but a 45° chamfer tool is used with a variable machining depth and a variable width guide since the cutting plane is no longer parallel to the X-Y plane.

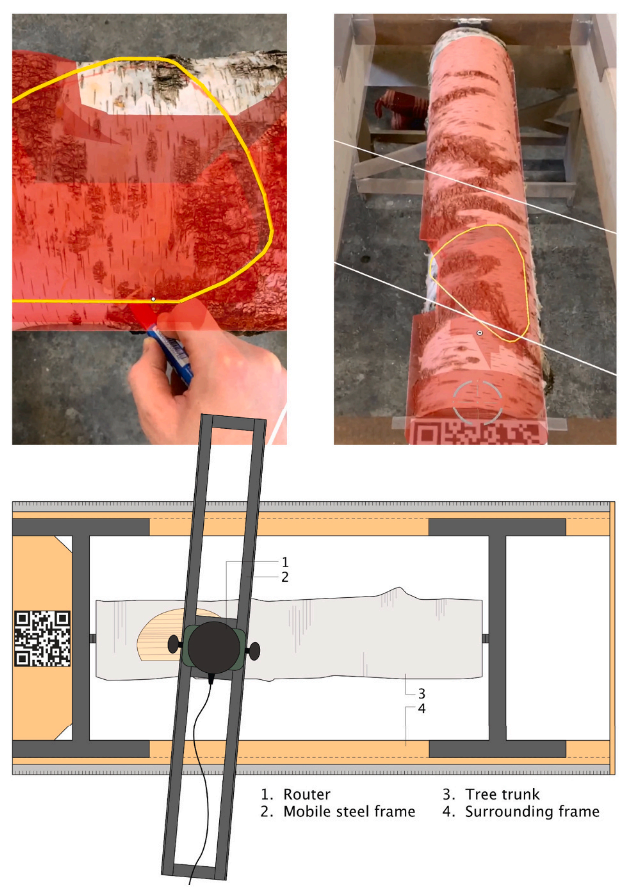

Fig. 3. Step 1, making type 2 cuts. Above: View from the smartphone's screen, with the 3D numerical model of the work piece and the contour of the area to be cut. Below: The router cuts inside the contour.

This experiment confirmed that "typical" machining, including CNC,

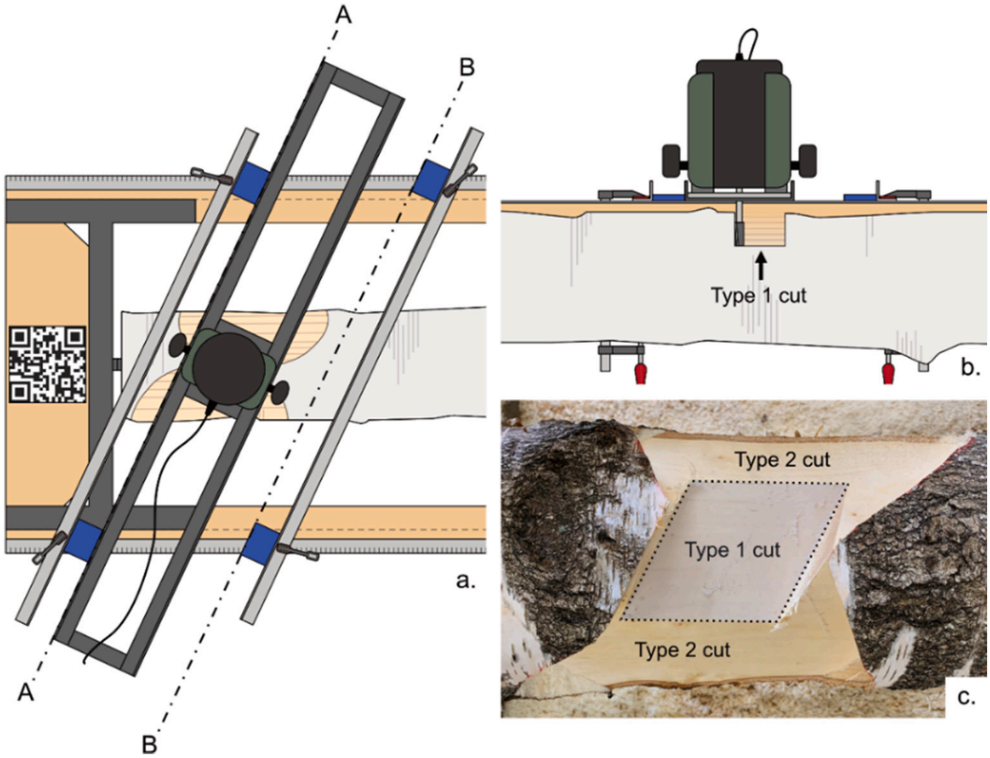

Fig. 4. Step 2, making the type 1 cut.

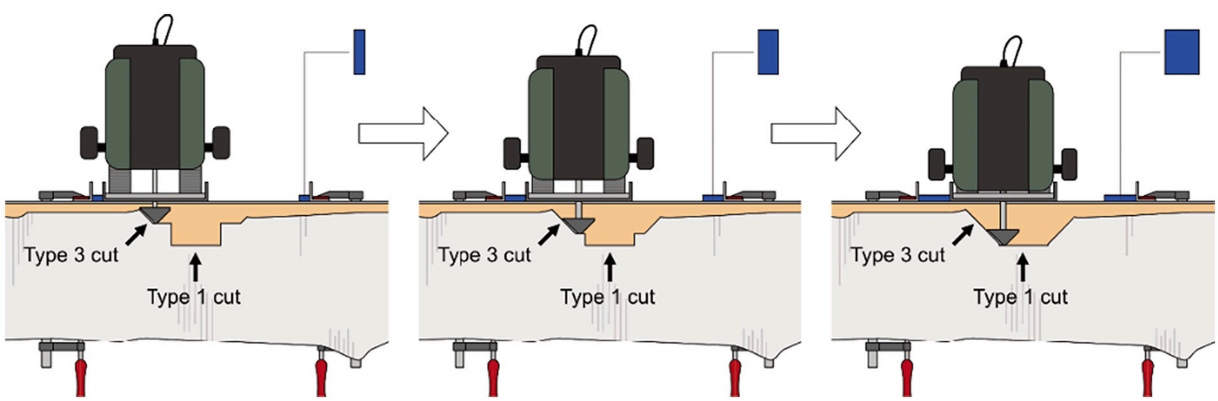

Fig. 5. Step 3, making type 3 cuts.

is not adapted to the machining of non-regular shapes such as tree trunks since it requires several movements of the workpiece, adequate and mobile supports, and several changes of reference, which has implications of lost time and increased errors. Furthermore, the lack of straightness of the trunks can generate either collision with the tool or inaccessible areas. In addition, the lack of degrees of freedom does not always allow for correct orientation of the machining in relation to the centroidal curve as shown on Fig. 6. Finally, the great length of the trunks is hardly compatible with typical cutting tools. All this justifies the relevance of a robotic arm associated to a specific reference system attached to the tree trunk itself.

2. State of the art

The state of the art includes many studies on reciprocal structures, on the use of robotics for construction, and on the use of sawn timber. Only some of these are cited herein. The use of logs for construction dates back millennia but has been abandoned in favor of concrete, steel, and squared timber that allow for much more flexible and efficient industrial processes. In recent decades there has been a resurgence of interest in timber with the development of robotics and digital tools that make it possible to consider for the first time the use of trunks in the construction of structures without the need for experienced craftsmen. However,

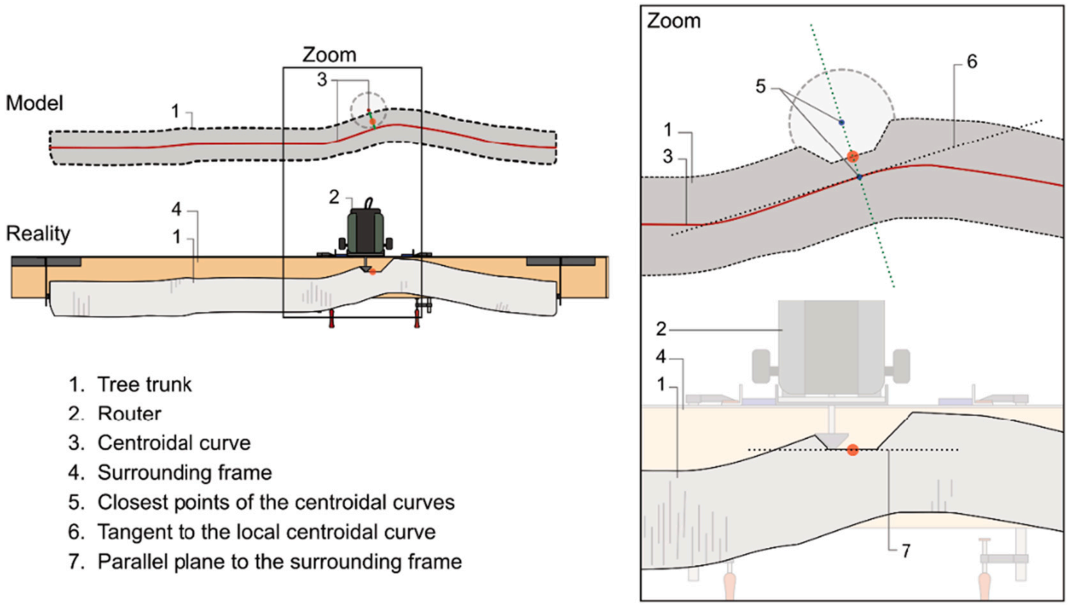

Fig. 6. Due to the lack of degrees of freedom, it is not possible in some cases to machine along the tree trunk's centroidal curve.

research is still needed in several areas and the state of the art is insufficient in several fields such as the mechanical characterization of trunks, the transmission of stress flows in trunk-to-trunk connections, the influence of trunk-to-trunk connections on the global behavior of reciprocal structures, the parameterization of trunk-to-trunk connections and the efficient transmission of data between digital tools and robots.

2.1. *Reciprocal structures and computational design methods*

The limited length of trunks is relevant in the consideration of reciprocal structures [7] (Figs. 7 and 8), also called nexorades [8]. These structures with members mutually supporting one another are of high architectural value and great antiquity. A reciprocal structure is a 2D or 3D structure formed by the repetition of one or more basic modules, following three essential rules [9]:

- A basic modulus is composed by at least three beams (Fig. 7).
- Each beam supports at least another one and is subjected to bending or compound bending depending on the shape of the structure.
- Each beam is supported by two others or by a beam and a support.

Beams of reciprocal structures can be assembled with bolted connections, but also without mechanical fastener by using pressure and friction [10].

Each beam supports neighboring beams and it itself is supported by neighboring beams [11], which creates non-hierarchical organization of beams that complicates the design of reciprocal structures. In other words, the position of each beam determines, and is at the same time determined not only by the position of the immediately adjacent beams, but also by all the beams of the structure [7]. The result of this specific organization is that the shape of a reciprocal structure is neither easy to control or predict [12]. During the last two decades, many researchers [2,13–18] focused on different algorithms of form-finding to explore the

Fig. 7. Basic reciprocal moduli with varying beam quantities.

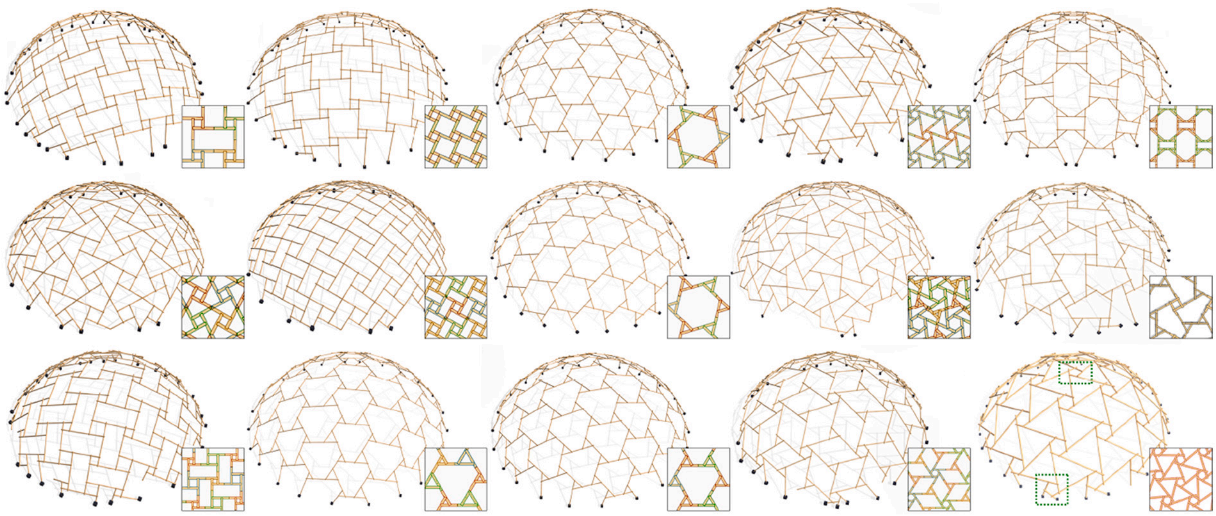

Fig. 8. Examples of reciprocal frames [11].

panel of possible arrangements while respecting specific geometrical constraints.

The complexity may not only lie in the form finding of the structures, but also in the specific connections between the beams, which could all be different. However, the evolution of parametric and computational tools such as Grasshopper [19,20], combined with the tools of CNC machining or robotic arms, makes it possible today.

2.2. Digital fabrication methods related to sawn wood

Beams with a rectangular section have been used in many projects including reciprocal structures and/or parametric design over the past decade. Some examples include Digital Wood Craft [21], Lamella Flock [22], Soundwave, Rheological Formation and Bodybuilding [23], which are all made with a 5-axis CNC. A 5-axis CNC was also used for the vertical structures Reverse Rafter [24] and Interlocking Spaces [25]. With the emergence of accessible robotic arms in recent years, it has become easier to achieve certain goals in terms of motions, possible tools, and detailed machining. In 2017, two 6 DoF robots were used to cut and assist in the connection of small components [26]. In 2012, Song et al. explored the design of a wooden frame without mechanical fasteners by using a global interlocking mechanism [27]. Godthelp et al. introduced a production process for regular patterned reciprocal frames without steel plate connectors [28] but with sectional reinforcement and self-drilling screws to account for when tensile forces occur at the node.

2.3. Wood logs and related digital workflows

The use of logs raises additional concerns because the centroidal curve is no longer a straight line, the cross-section varies, and there is no physical plane as it is the case for a sawn wood beam, which can be used as a reference plane. There are different ways to obtain 3D models of the logs like infrared scanners, photogrammetry, laser scanners, X-ray scanners, or computed tomography scanners, but photogrammetry is nevertheless the most cost-effective solution and was chosen for the *Wood Chip Barn project* [29].

Research has already investigated the possibility of using unconventional wood sections such as tree branches for the realization of structures, both from the point of view of design and fabrication [30,31] and from the point of view of numerical calculations of these structures [32,33]. Recently, tools such as sawmills [34,35], band saws [36–39], circular saws [40], claws [41], chisels [42], or milling tools [43–47] have been adapted to for the manufacture of complex 3D structures. Finally, robotic arms with 6 DoF (degrees of freedom) are beginning to be used because of their versatility of motion and wide range of tools. The roofs of the *Kijima Stonemason Museum* [13] and the *Hill Holt Wood* [48] are good examples of reciprocal frames composed of whole timber and steel connectors. The research project *Human in the loop* [49] uses an impressive audio-visual guidance system to machine the logs with a CNC router. Finally, Vestartas et al. has developed a joinery solver for the construction of structures made of round wood timber, the result of which was then tested with 6 DoF robots [50].

2.4. Mechanical characterization of logs

Knowing the mechanical characteristics of logs is essential for a reliable prediction of the structural SLS (Serviceable Limit State) and ULS (Ultimate Limit State) behaviors. The entire sawn timber industry uses the classification of element strength based on visual examinations and/or non-destructive tests, of which procedures are described in numerous standards. The resulting strength classes are associated with characteristic values, for example flexural strength and compressive strength parallel to the fibers, which allow for a reliable SLS and ULS calculation of the structures based on a statistical approach. Such standards for the mechanical characterization of timber logs are rare and are often not detailed enough to guarantee reliable results or are only applicable to tree species from that country. In a study concerning the evaluation of the mechanical properties of small-diameter logs, Wolf & Moseley [51] detail the problem of developing adequate design standard. However, the American Society for Testing and Material (ASTM) have published some standards such as the ASTM D25 (Standard Specification for Round Timber Piles), ASTM D2899 (Standard Practice for Establishing Allowable Stresses for Round Timber Piles), ASTM D3200 (Standard Specification and Test Method for Establishing Recommended Design Stresses for Round Timber Construction Poles) or ASTM D3957 (Standard Practices for Establishing Stress Grades for Structural Members Used in Log Buildings).

Others have tentatively tried to define the mechanical properties of whole timber, such as a project conducted in the 1990s in Europe [52], during which many trunks of different species were tested (Scotch pine, Norway spruce, Sitka spruce, larch, and Douglas fir) with destructive and non-destructive methods (visual grading, static bending, longitudinal stress wave and X-ray). The study presents a statistical analysis for the dependence of strength and stiffness on different factors such as density, knots, moisture content, diameter, and age to find a correlation between these values and the mechanical resistance. The New Zealand company Unilog [53] has a promising approach: "Proof-testing is carried out at the very beginning of the manufacturing process, with no damage to the pole, and immediate results available. Proof-testing involves loading a pole into the pole testing rig, applying a proof force by way of a hydraulic ram to achieve the required force in 3-30 seconds, and maintaining the proof force for at least 15 seconds with the pole showing no signs of distress. Modification factors to account for characteristic stresses are applied in accordance with NZS3603:1993 Timber Structures Standard".

3. Methodology and results

3.1. Centroidal axis and centroidal curve

Tree trunks cannot be considered as perfect truncated cones and even less as perfect cylinders, as shown in Fig. 9.

The centroidal axis is defined as the linear regression line of mesh points derived in Grasshopper. Fig. 10 illustrates how this is found with points R and S representing the intersection between this line and the mesh. The centroidal axis is used for the design of the structure, explained in section 3.2.

Connection definitions and their geometric parametrization, such as those detailed in section 3.5, require the assumption that where two trunks are connected, they can be approximated by their two respective inscribed circles of diameters ϕ_1 and ϕ_2. In a trunk, the curve which links all the geometrical centers of these successive inscribed circles will be called "centroidal curve". Fig. 11 shows how this curve is found. This concept of the centroidal curve is also useful in the calculation of internal stresses because it allows one to approximate the trunk by a series of successive cylinders (Fig. 12).

3.2. General approach

This methodology is validated with respect to connections between trunks, no matter the structure type: simple structures such as floors made of primary and secondary beams, stacked wooden structures, or more complex structures such as reciprocal structures. To validate this methodology, a full-size reciprocal structure consisting of 14 trunks was constructed (Fig. 38). This structure can be seen on the following videos: click here [54] and here [55]. The construction of such a reciprocal structure was a complex way to validate the approach, but it is the approach that allowed more universality as the connections of a reciprocal structure are all different. Its design and fabrication process were split into three main steps, as shown in Fig. 13.

In step 1, each trunk is photogrammetrically scanned using Metashape [55] and a library containing the 3D mesh of each trunk is created (Fig. 14). The 3D models are then analyzed to extract geometric data such as the centroidal axis and the centroidal curve of the tree trunks.

Cutting trunks with a robotic arm requires the selection of a Cartesian coordinate reference system with the X, Y, and Z axes, assigned to each trunk. This requires one to choose 3 points on the log and to transfer them to the 3D model, or vice versa. This is discussed in section 3.3.

Step 2 concerns the design of the reciprocal structure itself and the definition of the connections, which is done with Grasshopper and Rhino software and is summarized in Fig. 15. Data input for each connection includes the 7 parameters detailed in section 3.5.

A schematic representation of the prototype structure is first predefined considering the basic design rules of reciprocal structures

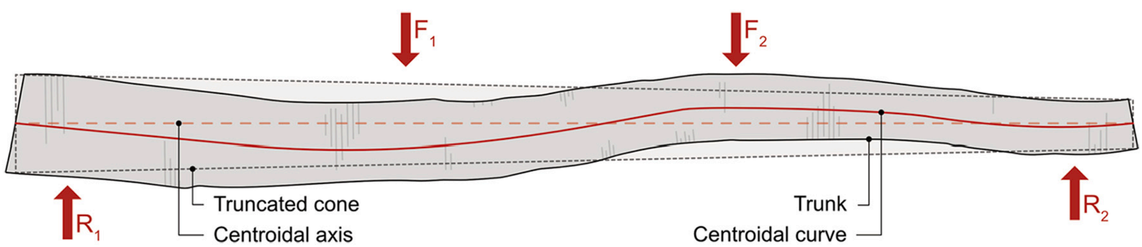

Fig. 9. Comparison of perfect truncated cone with centroidal axis, and irregular geometry tree trunk with centroidal curve.

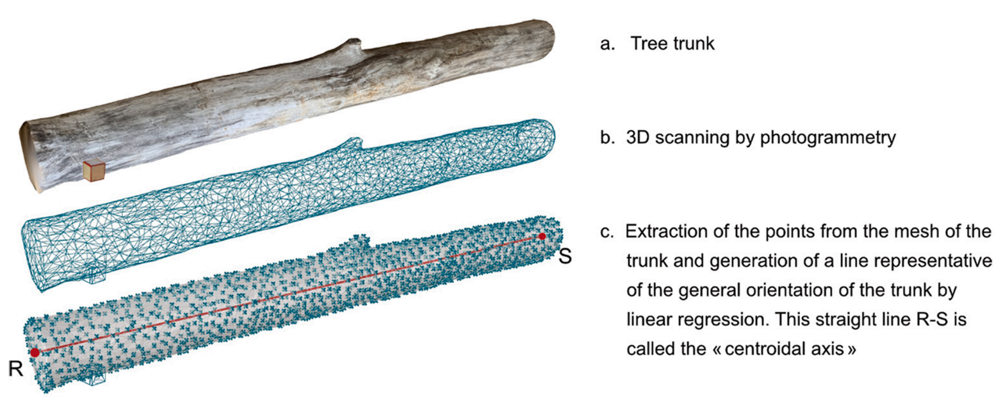

Fig. 10. Definition of centroidal axis R-S for assignment of a straight axis on trunks of irregular geometry.

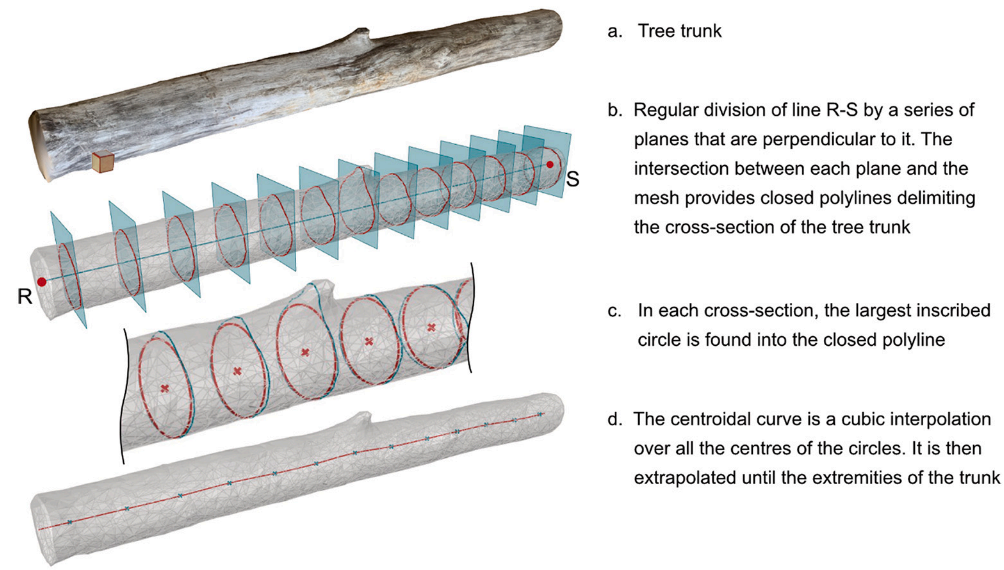

Fig. 11. Demonstration of the centroidal curve, which is not a straight line, passing through the geometrical center of the successive circles inscribed into the trunk.

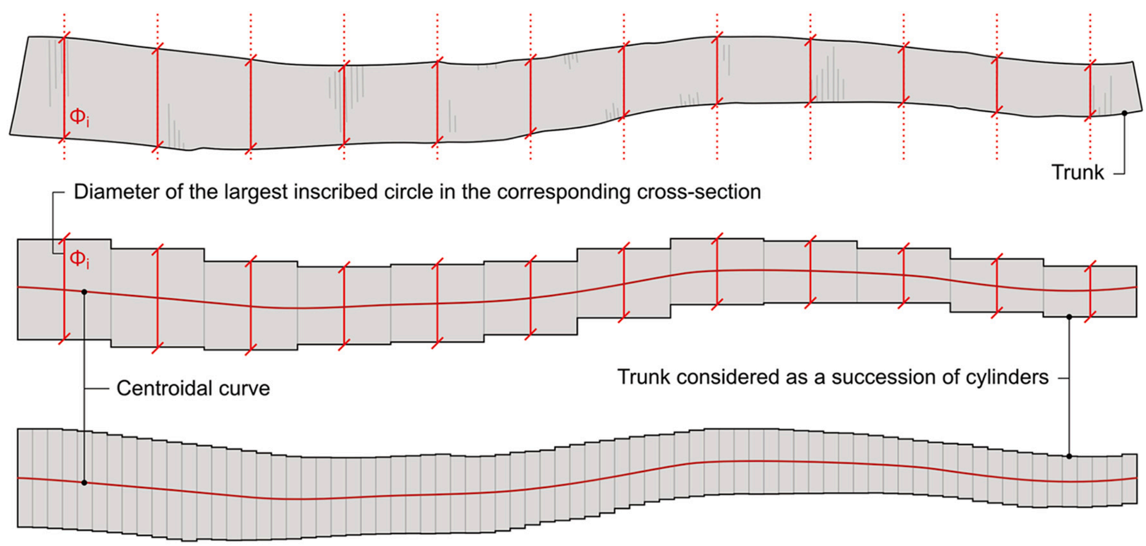

Fig. 12. Approximating a trunk with a cylindrical series to enable (i) Connection design according to the parameters defined in section 3.5 and (ii) More precise calculation of a trunk's internal forces and stresses.

(Fig. 15a). Each trunk is represented by its centroidal axis and for any given connection, the parameter "O" represents the distance between the centroidal axes of the trunks (Fig. 15a). Similarly, the parameter "E" defines the distance between the centroidal curves, which means that if the value of "E" equates the value "O" it is indicative of a perfectly straight specimen.

The form-finding process of the reciprocal structure can be achieved in two ways: either the form-finding is performed directly accounting for the exact 3D geometry of the logs with variable diameters and curvatures (centroidal curves and parameters E), or the form-finding is defined with logs represented by straight axes (centroidal axis and parameter O). In the first case, the form-finding algorithm of a reciprocal structure is complex and constitutes a separate research topic which is beyond the scope of this research. In the second case, the form finding is simplified, but it requires the assumption that the curvatures of the logs are small. The form finding can be performed with different values of an offset "O" specific to each connection. For the prototype described in section 4, logs had similar diameters, and a single average value of the offset "O" was chosen. Typically, for a connection between two trunks of respective diameters ϕ_1 and ϕ_2, a value of $O = (\phi_1 + \phi_2)/4$ is reasonable. Once parameter "O" has been calculated for each connection, the shape of the reciprocal structure is fixed and the 3D models of the trunks are imported into the Grasshopper script, which enables calculation of parameter "E" for each connection. A large difference between O and E indicates that a curvature is too big and a physical intersection of two trunks cannot exist, which can be addressed by either rotating the trunks or changing the initial offset "O".

The 3D mesh geometry of each trunk is associated to a well-defined local (X, Y, Z) coordinate reference system (see section 3.3). This enables each mesh geometry to be easily linked to the global coordinate system of the reciprocal structure. This means that through the Grasshopper design interface any trunk can be rotated as needed. In fact, if the process assumes a limited curvature of the trunks, the angular position of each trunk in the Grasshopper interface is relatively negligible. For the prototype described in section 4, the trunk meshes were imported with an arbitrary angular position (Fig. 15b).

Finally, the cutting volumes are calculated and the BTL exchange file for the robot is created (Fig. 15c). The principle of the BTL file is

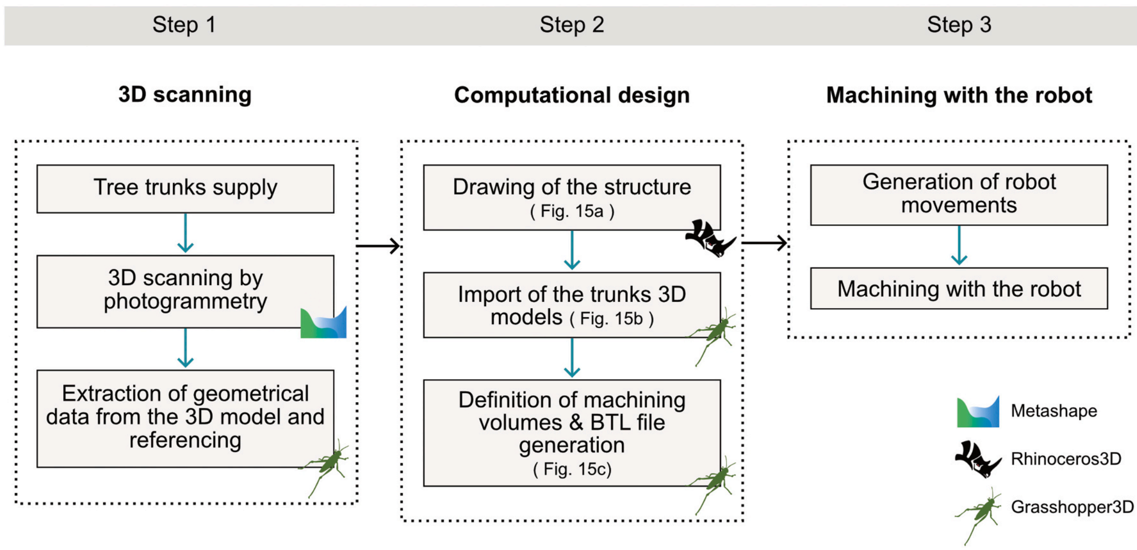

Fig. 13. Design and fabrication process of a structure composed of tree trunks and machined with a 6 DoF robotic arm.

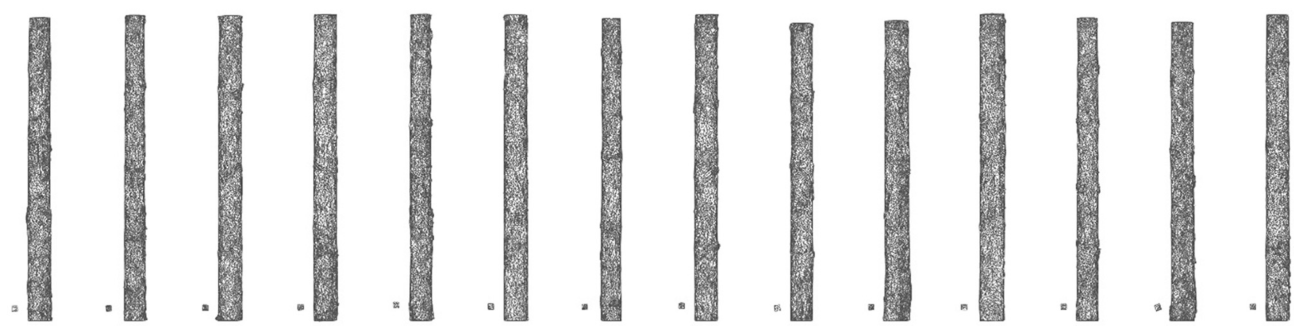

Fig. 14. 3D model photogrammetry scans of the 14 tree trunk elements of the prototype.

explained in section 3.7.

Step 3 is related to the machining of each trunk with the BTL file as input data, which requires the BTL file to be converted into movement instructions for the robot arm.

3.3. 3D scanning and reference system

For this prototype, the 3D scan was performed with photogrammetry. This process requires human intervention for post-processing, and it is slow, but it has the advantage of accuracy to the millimeter without high-tech equipment. Agisoft's Metashape [56] was used to obtain 3D mesh of each tree trunks positioned vertically such that photos could be taken from all angles (Fig. 16). About 40 pictures per trunk were required to cover all angles with sufficient overlap to ensure the reconstruction of the model. To limit the size of the 3D models, the mesh resolution was set at 1000 faces per meter of log, which was sufficient.

To make accurate cuts on a geometrically imperfect object, such as a trunk, it is necessary to associate it with a local coordinate reference system (X, Y, Z). This requires one to choose 3 points on the log and to transfer them to the 3D model, or vice versa. The process that was used for the prototype is described below, and an alternative process is provided in the discussion of section 4.

For the prototype that was constructed (section 4), the X-axis used was the centroidal axis. Furthermore, before the 3D scan of each trunk, a 60 mm cubic box, large enough to be modelled photogrammetrically, was attached at one end with a screw which remained attached to it during the entire process, from 3D scan to robotic cutting. The geometrical center of the box (or the head screw) and the centroidal X-axis define the X-Y plane (Figs. 17 and 18) and thus the entire (X, Y, Z) Cartesian coordinate reference system.

Once the Cartesian coordinate reference system is assigned to the tree trunk, it is referenced for all cuts. In practice, the cutting procedure is as follows, and its relevance, advantages and disadvantages are discussed in section 4:

- Place the trunk on its supports. The trunk is previously equipped with the small cubic box for which the position must stay unchanged after the scan.
- Mark the R and S points with a marker. To achieve this, the shape of each end is printed out on a 1:1 scale from the digital model of the trunk, together with the position of the R and S points (Fig. 18d).
- The tool central point (TCP), described in section 3.7, is placed on points R and S (Fig. 18d) and on the head of the screw which maintains the box (Fig. 18e), allowing the robot's head to record the coordinates of these 3 points (point R is assigned coordinates (0,0,0)).
- The robot, whose instructions are sent to it according to this Cartesian coordinate reference system, can then start machining.

3.4. Search for a suitable trunk-trunk connection

As explained in the Introduction, stacked wooden cottages are an interesting source of inspiration for the design of connections between logs, as shown in Fig. 1 [5], but most of these constructions are built with calibrated logs and not with raw logs.

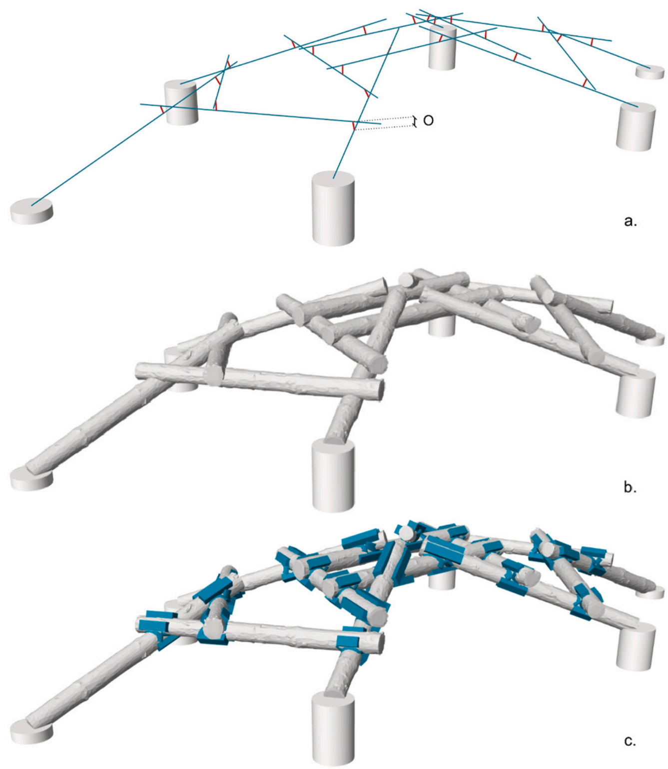

Fig. 15. Details of step 2; (a) Accounting for the basic design rules of reciprocal structures, a schematic representation of the structure is made with the centroidal axes of the trunks, (b) Import of the trunks' 3D meshes (c) Calculation of the cutting volumes and creation of the BTL file.

The search for the optimal shape, size, and position of the notches in a connection between a supporting and a supported trunk is a complex exercise that must consider many parameters. This search is complicated by the irregular shape of the trunks and the cutting limitations of typical machining tools. Further considerations include effective transmission of stresses between the supported and supporting beams, curing the timber and possible shrinkage, possible presence of tensile stresses perpendicular to the fibers, the desire to facilitate ease of interlocking, the specificity of the cutting tools, and the on-site construction sequencing.

The support of any beam is assumed to be articulated but locked in translation in all directions. If the structure is designed in such a way that the resultant force is orientated from the supported beam to the supporting beam and, under the assumption of frictionless contact, at least 4 planes are required to block the three translations in the notch. In addition, a conical shape is necessary for 4 reasons:

- To facilitate nesting, and thus facilitating the construction of the structure. Particularly with respect to the installation of a reciprocal structure, closing of a module requires a rotation of the last element around the others, and thus of the inclined faces in the connection.
- To Minimize the influence of the lack of precision of the cutting tools.
- To allow for dimensional variation of the wood as it changes in humidity, while keeping the faces in contact with each other, as shown in Fig. 19. However, due to the anisotropy of wood, a variation of humidity will transform theoretical cross sections into non-regular shapes, with consequences of (i) faces will come into contact with each other after local yielding and (ii) friction stresses could prevent the movement of one beam over the other and modifying the flow of stresses must be quantified.

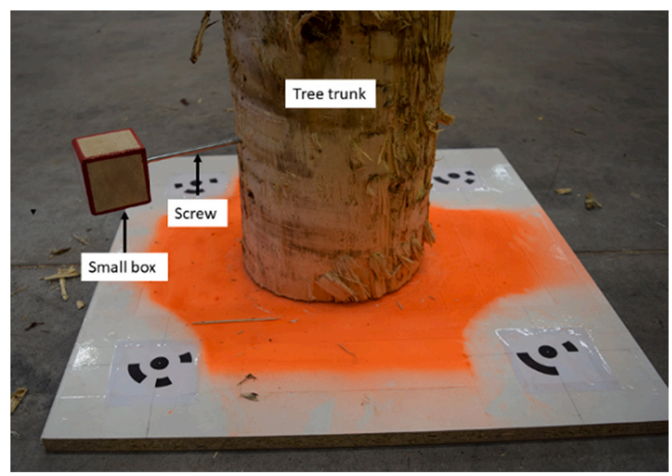

Fig. 17. To define the Y and Z axes, a long screw with a small 60 mm box at one end of each trunk is placed, large enough to be modelled photogrammetrically.

Fig. 16. Orientations of photos taken for 3D scan with photogrammetry, taken with a Nikon D5300 using a Nikon AF-S DX NIKKOR 18–55 mm f/3.5–5.6G VR II camera lens.

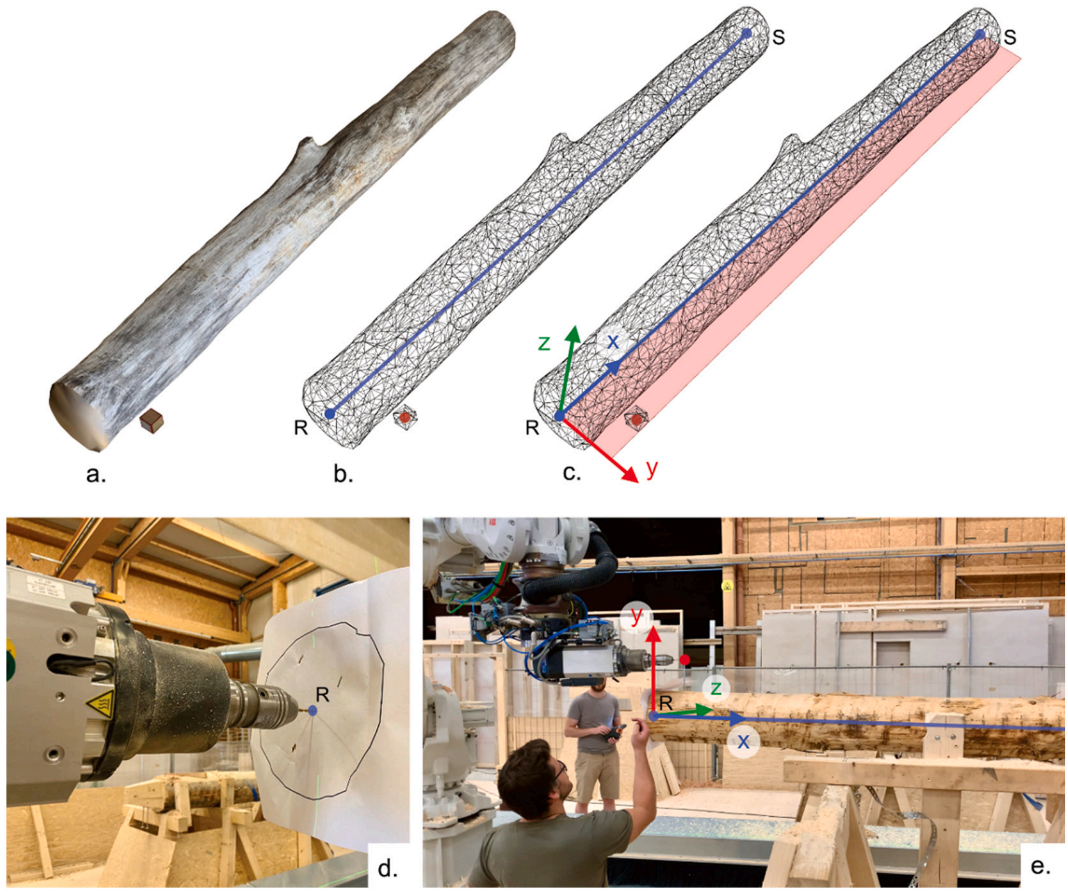

Fig. 18. Placement of the origin of the Cartesian coordinate reference system, definition of the X, Y and Z axes, and directing of the robot to point R, point S, and the head screw.

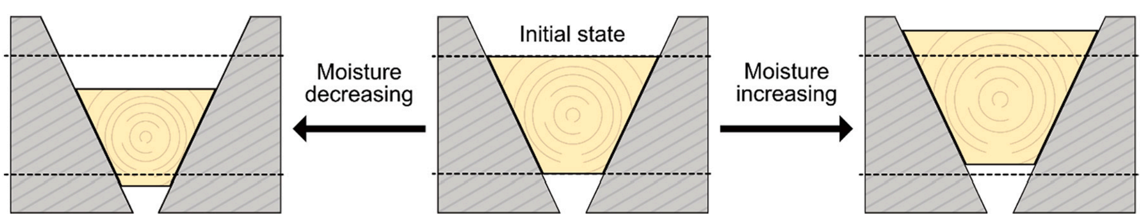

Fig. 19. Conical shape allowing nesting and movement in response to changes in humidity.

- To avoid stresses perpendicular to the fibers, which timber often cannot withstand without cracking. This is illustrated in Fig. 20 where scenario 20d is ideal since it avoids contact between horizontal faces which ensures that there are no tensile stresses perpendicular to the fibers, unlike the scenarios shown in Fig. 20a and c.

Finally, the notch must be robot compatible. In other words, it must be simple and wide enough to allow easy access to the cutting tools.

The notch developed and parameterized in section 3.5 is defined by 5 cutting planes shown in Fig. 21:

- Type 1 cut: The main (horizontal) plane is never in contact with another plane to avoid tensile stresses perpendicular to the fibers, as explained previously (Fig. 20), but also to maintain good interlocking when humidity variations create dimensional variations. This plane is at point C and is perpendicular to line AB (Fig. 22) which represents the minimum distance between the two centroidal curves of the beams. Point C can be located elsewhere than in the middle of segment AB, depending on the distance between the two beams, their respective diameters, and their load levels (see section 3.5).
- Type 2 cuts: Planes are inclined and parallel to the centroidal curve of the beam. A type 2 cut of a trunk is in contact with the type 3 cut of the adjoining trunk, and vice versa.
- Type 3 cuts: Planes are parallel to the centroidal curve of the adjoining beam. A type 3 cut is in contact with the type 2 cut of the adjoining beam, and vice versa.

To avoid weakening sections, it is assumed that the beams are never notched beyond their radius. In the remainder of this article, a connection with such notches is referred to as a “JJP connection”.

3.5. Parameterizing the geometry of the JJP connection

Keeping in mind that the individual geometry of the trunks, as well as their respective orientations and diameters, can be all different, the seven geometric parameters that characterize the JJP connection:

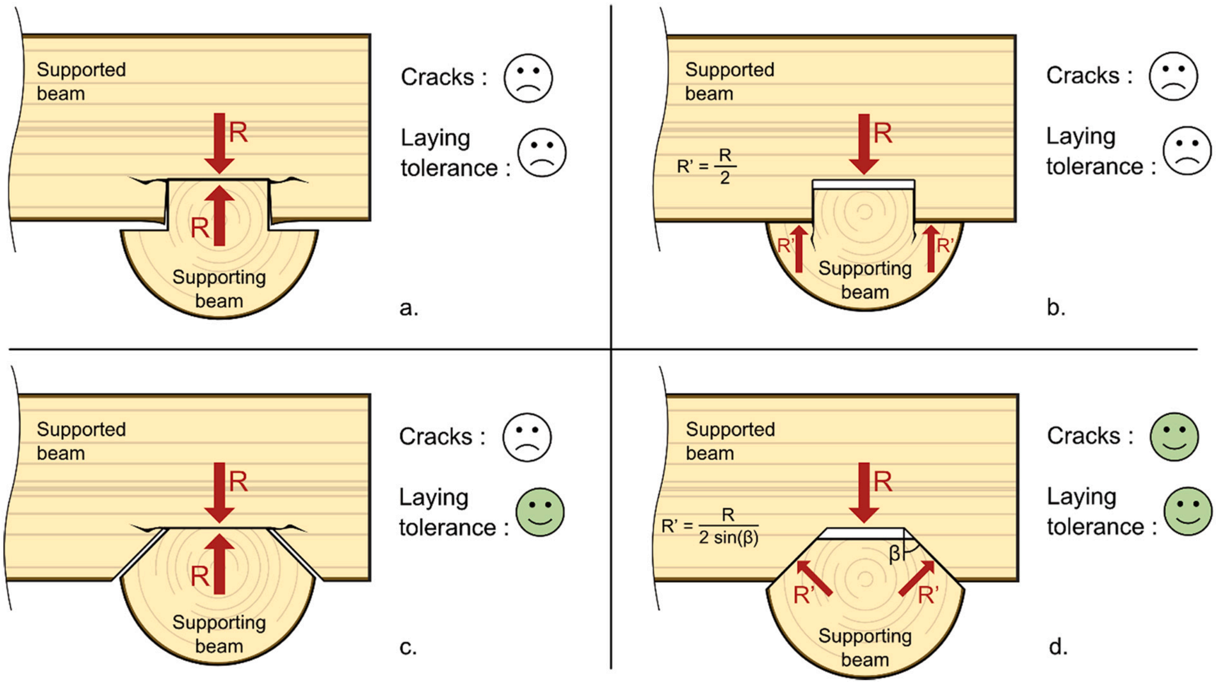

Fig. 20. Possible interface scenarios where scenario *d* combines the advantages of a conical shape and the elimination of tensile stresses perpendicular to the fibers.

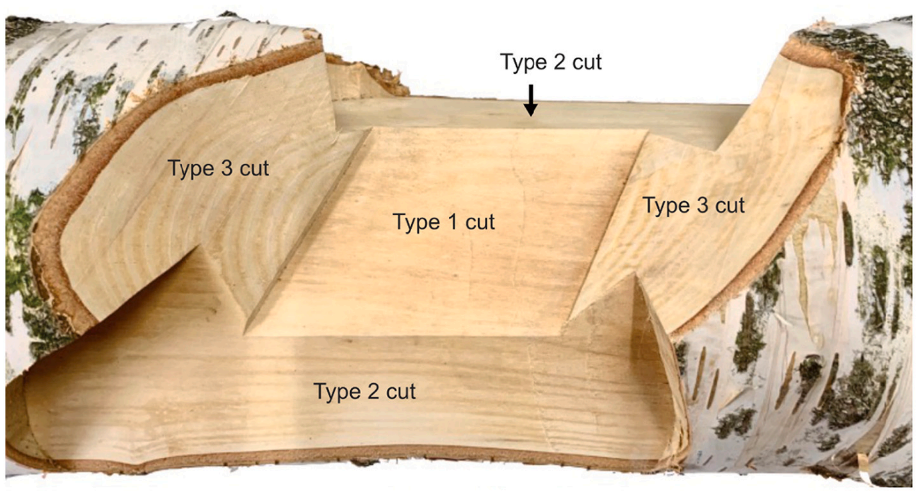

Fig. 21. A notch is defined by 5 cuts where each cut has its main plane.

eccentricity (E), notch depth parameter (μ), penetration angles (β1 and β2), Penetration ratio (λ), Bottom offset (B_O), and Cutting offset (C_O). These can be found using the following six respective descriptions:

(i) The global eccentricity E: E is the smallest distance |AB| between the centroidal curves of two beams in contact with each other (Figs. 22 and 23), while O is the smallest distance between their centroidal axis (as explained in section 3.2 and shown in Fig. 15a). In other words, E is equal to O if the adjacent trunks both are perfectly straight, which means that the centroidal axis and the centroidal curve are identical. Point A is the point included in the centroidal curve of beam 2, closest to the centroidal curve of beam 1, and vice versa (Fig. 22). The parameter E defines the location of the notches and influences the shape and appearance of the whole structure.

The selection of the value of E should also be made according to the forces in the beams, the stresses between the connection faces, and the quality of the nesting. If E is small, a trade-off exists because beams are heavily notched and this results in local weakening, but the interlocking is better and as the total thickness of the beam at a connection location decreases, the contact surfaces increase, which facilitates the transmission of the compressive stresses.

It is important to understand that the parameter E is dependent on the selection of the parameter O. To change the value of E for a connection, one must change of the value of O, which influences the overall shape of the structure. The process can thus become iterative.

(ii) Position μ of the type 1 cut: The beams are never notched by more than their radius to avoid critical weakness, and the height $|L^+L^-|$ in which the type 1 cut (point C, Fig. 22) can be placed is variable, and shown in Fig. 24. The height $|L^+L^-|$ depends either on E, or on the diameters ϕ_1 and ϕ_2, or on all three, with $|L^+L^-|$ being taken as the minimum of (E, $\phi_1/2$, $\phi_2/2$, $(\phi_1+\phi_2)/2$-E). Parameter μ is defined as $\mu = |L^+C|/|L^+L^-|$, with $0 \leq \mu \leq 1$. For “normal” situations such as those shown in Figs. 24c, e, f, h, and i, a value of μ close to zero means that the

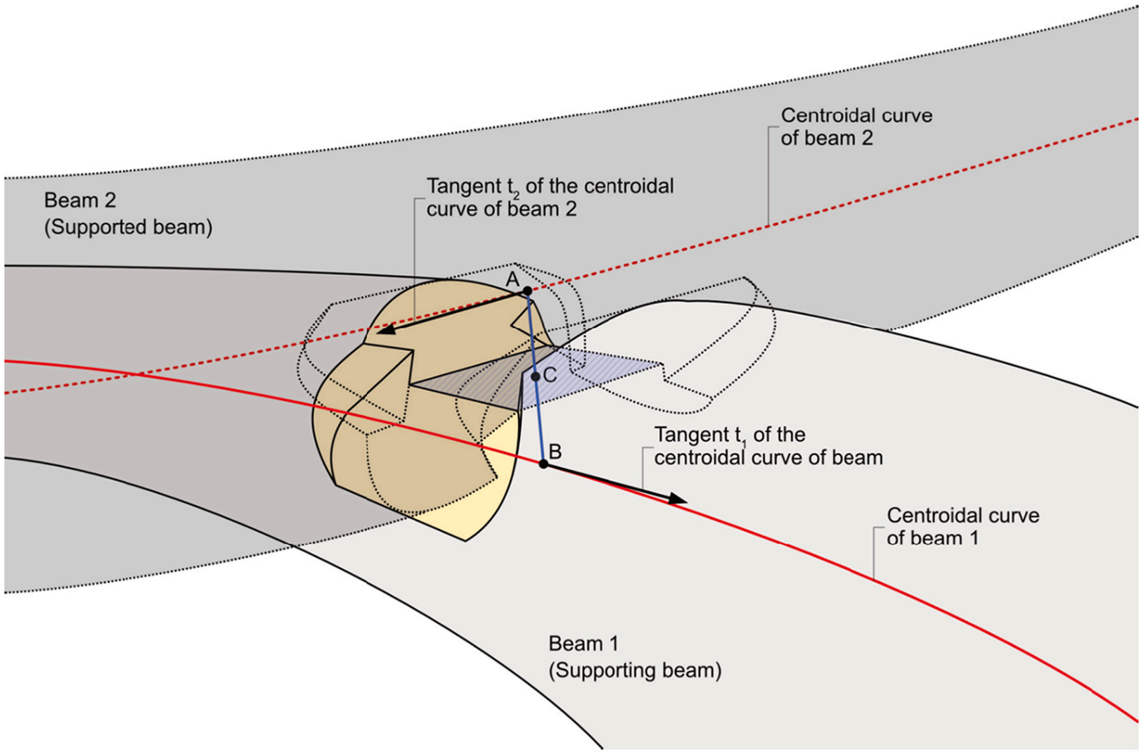

Fig. 22. Schematic 3D view of the connection between 2 trunks.

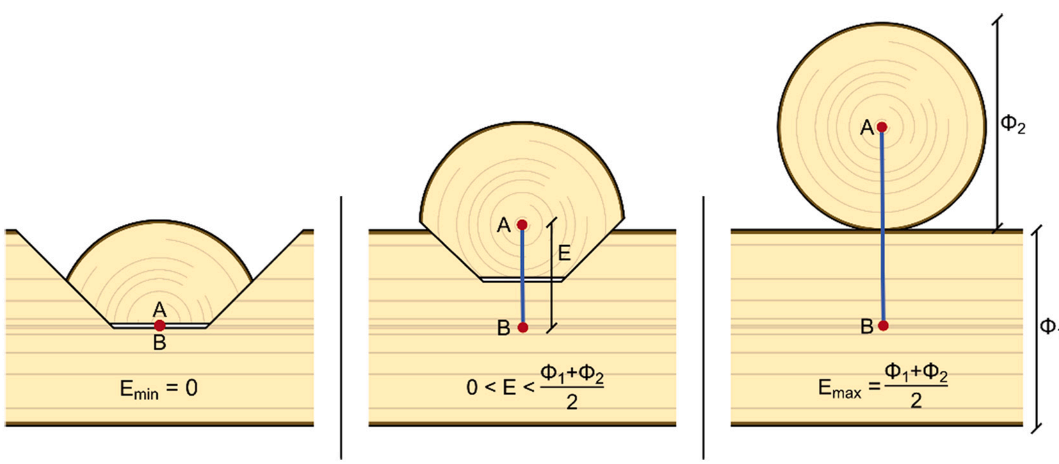

Fig. 23. The parameter E is the minimum distance between the centroidal curves of two beams in contact with each other.

supporting beam is lightly notched, and the supported beam is heavily notched. On the contrary, a value of μ close to 1 means that the supporting beam is heavily notched, and the supported beam is lightly notched. The parametric design process is the following and is summarized in Fig. 25: (i) Eccentricity E is chosen with the condition $E < (\phi1+\phi2)/2$ and parameter μ is "arbitrarily chosen" between 0 and 1, (ii) The value of $|L^+L^-|$ and $|L^+C| = \mu|L^+L^-|$ are calculated, and (iii)|AC|, |CB| and/or other distances can be easily calculated for drawing, programming, and sending instructions for machining.

Just as for E, the choice of the value of μ should also be made according to the forces in the beams, the stresses between the connection faces, and the quality of the nesting. In view of the above considerations and without precise information about the orientation of the forces to be transmitted from one beam to another, a value of $\mu = 0.5$ is the recommended value.

(iii) Penetration angles β_1 and β_2: The penetration angles are defined in Fig. 26 and are visible in Fig. 21. The value of these angles must be selected according to various factors. A large value of β facilitates an easy interlocking, a better transmission of compression stresses and a

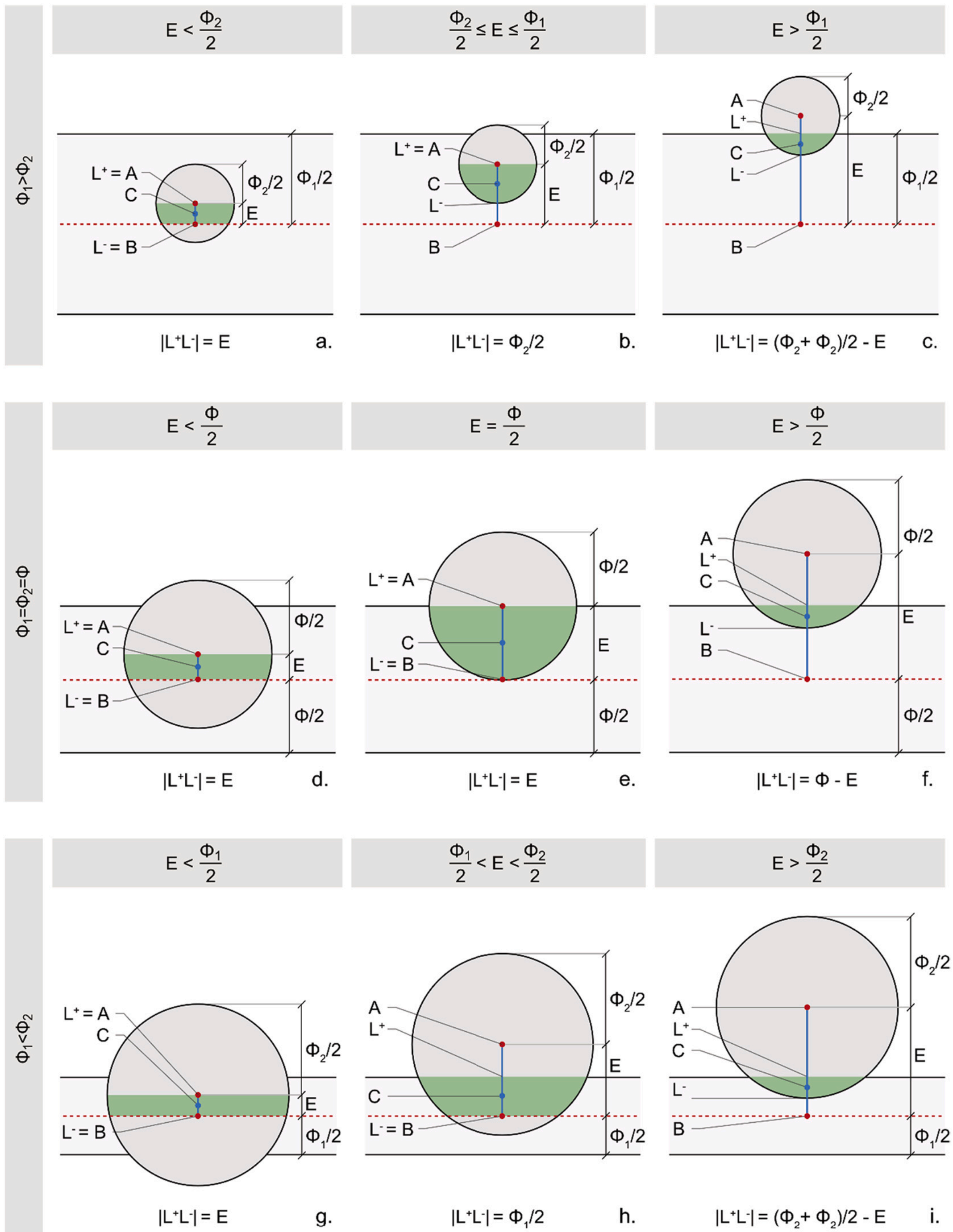

Fig. 24. Parameter $\mu = |L^+C|/|L^+L^-|$ $(0 < \mu < 1)$ defines the position of the type 1 cut.

good behavior with humidity changes, but the inconvenient risk is that the supported beam might "roll" on the supporting beam, as shown in Fig. 27. Without precise information about the orientation of the forces to be transmitted from one beam to another, a value of $\beta_1 = \beta_2 = 45^\circ$ is the recommended value. While not always necessary, note that to prevent joint dislocation a metal connector, such as a lag bolt, can be inserted through connections after the structure is built to avoid complicating assembly and sequencing.

(iv) Penetration ratio λ: The penetration ratio λ is defined in Fig. 18, with $\lambda_{1\,or\,2} = d_{1\,or\,2}/(\phi_{1\,or\,2}/2)$

Once again, the selection of the value of penetration ratio λ influences the transmission of forces and stresses into the connection and must be chosen wisely. Fig. 28 shows that, for $E > (\phi_1+\phi_2)/2$, the ideal

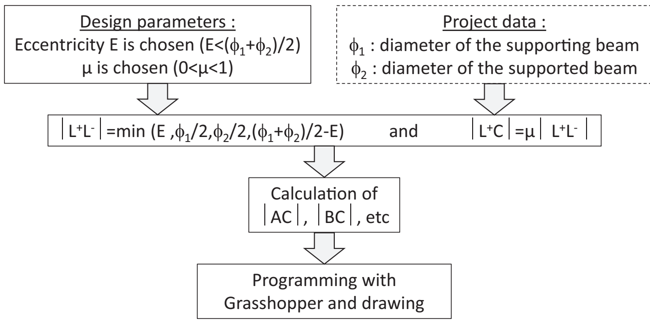

Fig. 25. Selection of parameters E and μ allows knowledge of the exact position of the trunks, facilitating Grasshopper illustration, and generating trunk intersection.

scenario is a value of lambda such that the type 3 cuts originate at the point of intersection F between the circumference of the supported beam and the upper fiber of the supporting beam. In this case particularly, the cross-section of the supported beam is notched as little as possible while having the maximum contact area between the type 3 cuts. For $E < (\phi_1+\phi_2)/2$, a value of λ must be found that is neither too small to avoid a weakening of the cross-section of the supported beam, nor too large to avoid reduced contact areas on the type 3 cut.

(v) Bottom offset B_O: As explained above in section 3.4, Fig. 20, a free space must be provided to avoid contact between the type 1 cuts of each trunk, as shown in Fig. 29, which includes correct interlock between the two beams, good contact between the inclined faces, and avoiding tensile stresses. The way the cross section of the log will deform while drying depends on the parameters E, μ, β, λ and the timber species. However, an approximation of the thickness B_O of this space can be obtained by considering the variation of the diameter ϕ of a log: $B_O = \alpha w \phi$, where α is the radial hygrometric shrinkage or swelling coefficient (maximum 0,2 [%/%]), and w the variation in the water content of the wood. Considering that the wood is cut during its "green" state, and that its water content can reduce to 7%, $B_O = 46.10^{-3}\phi$ is obtained where Table 1 gives the recommended values for B_O for different diameters.

(vi) Cutting offset C_O: The offset C_O plays an important role during the assembly of a structure, by allowing a rotational movement when a supported beam is placed. This is particularly important for the closing of reciprocal modules where the insertion of the last beam of a module is

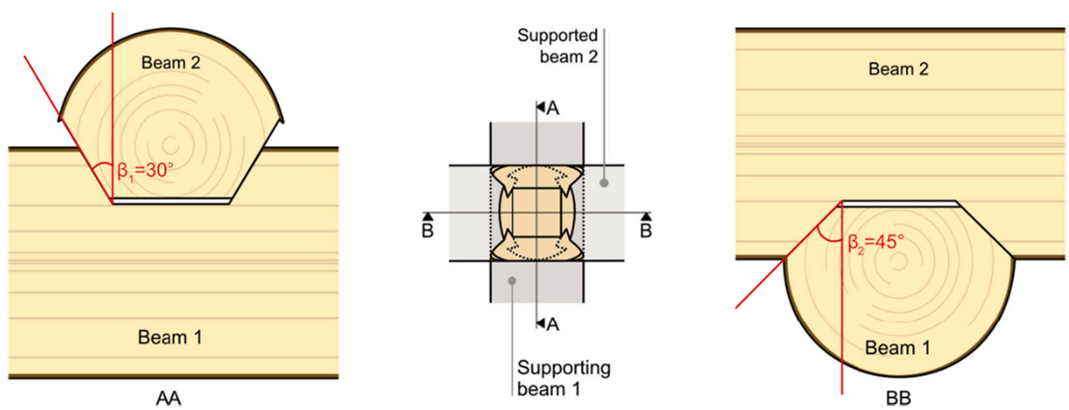

Fig. 26. Penetration angles β_1 and β_2.

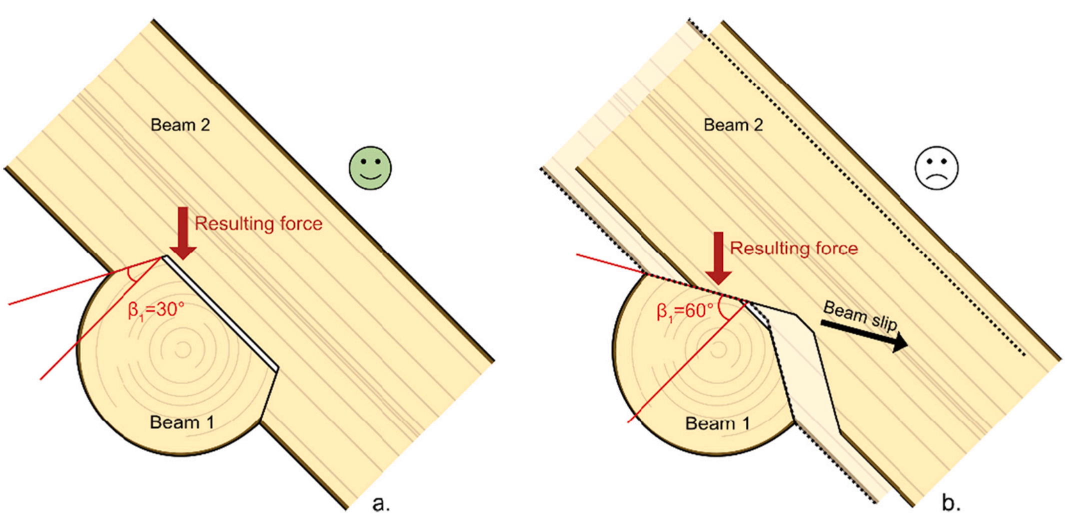

Fig. 27. If angle β_1 or β_2 is too large, the supported beam risks rolling over the supporting beam, therefore scenario (a) is more stable than scenario (b).

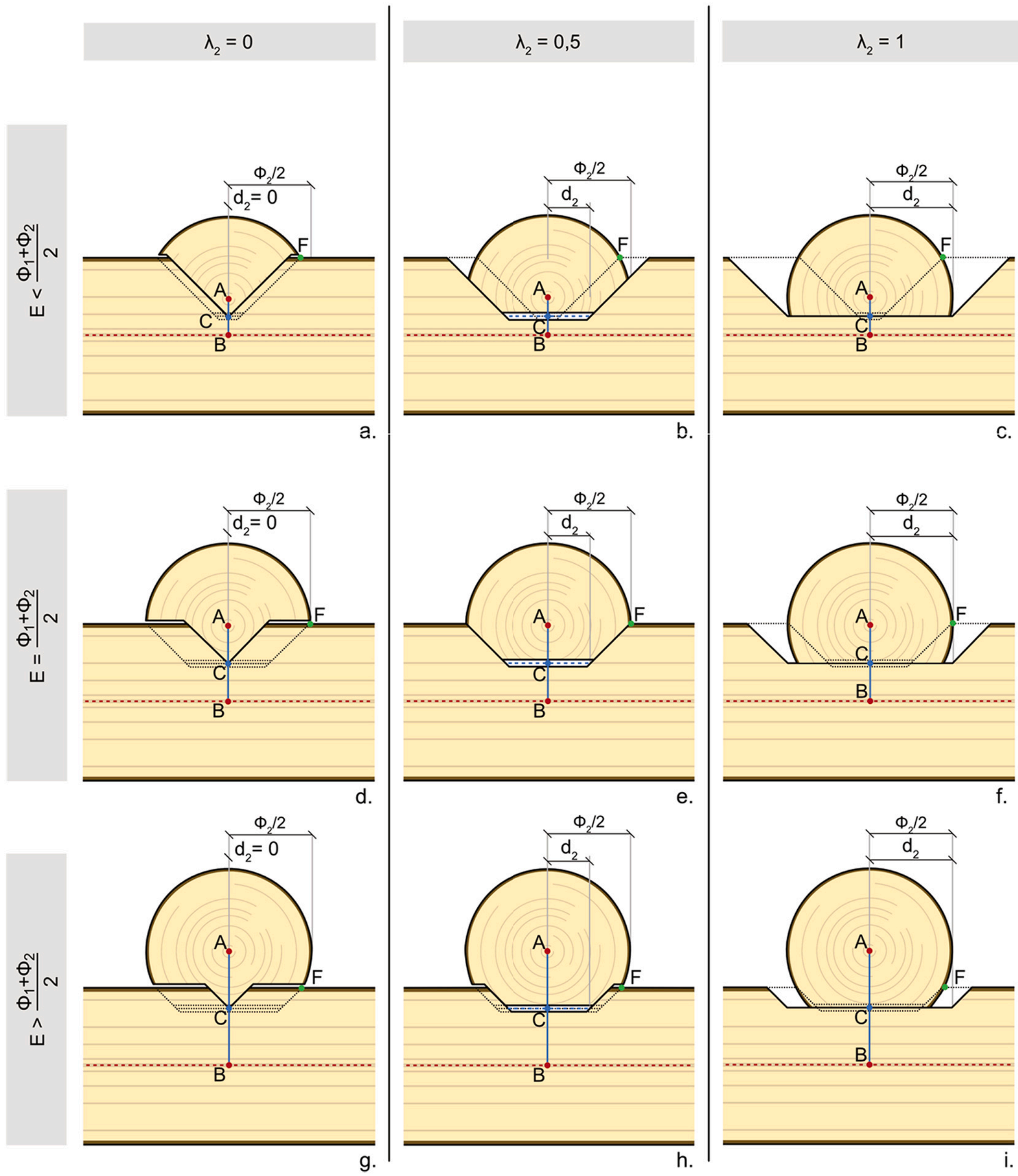

Fig. 28. Various configurations that illustrate the concept of penetration ratio λ (with $\phi_1 = \phi_2$, $\beta_1 = 45^\circ$ and $\mu = 0.5$). Note that some do not correspond to relevant technical solutions, i.e., cases c, d, f, g, i.

difficult if there is not enough tolerance in the connection. The cutting offset C_O is also necessary to reduce the consequences of machining inaccuracies or the presence of a log protrusion that could locally interfere with the connection. As shown in Fig. 20, the negative effect of the offset is to reduce the surface area of the type 3 cuts, which is unfavorable in the proper transmission of compressive stresses. The value of the offset should therefore be limited to the strict minimum. The experiences building this structure, shown in Fig. 1, prompt that a recommended cutting offset equal to $\phi/10$ is sufficient and can even be smaller for more "classical" structures such as floors.

3.6. Computational design with grasshopper

Fig. 31a shows the graphical result of the script developed on Grasshopper. Fig. 31b shows the general principle of the script, which allows a design according to the structural rules of reciprocal structures, a design of the JJP connections (all different from one another), and the production of a BTL file that can be used by the robot for cutting (BTL is

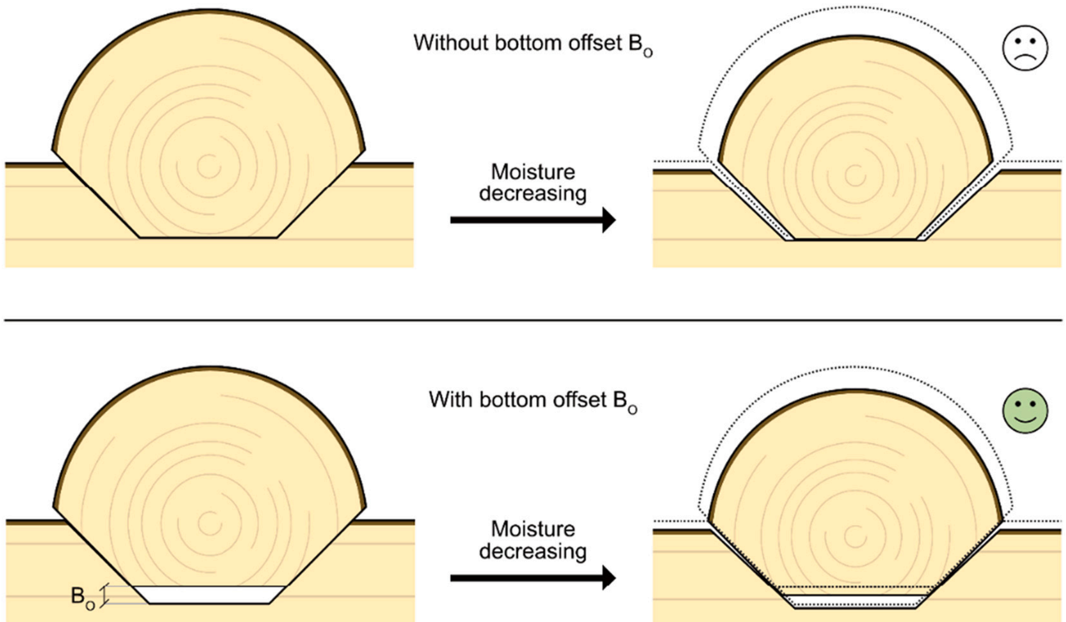

Fig. 29. Definition of the bottom offset B_o.

Table 1
Recommended values for $B_{o.}$

Log diameter ϕ (cm)	B (mm)
20	9
30	14
40	18
50	23
60	28
70	32
80	37

detailed in section 3.7). Fig. 31c shows the Grasshopper interface of the connection design. In this chapter, how Grasshopper script manages the design of connections between trunks is described.

The design of each connection includes three steps:

- Step 1 (refer to Fig. 22): For each JJP connection, the closest points A and B between the centroidal curves of the two trunks are calculated, as well as the corresponding diameters ϕ_1 and ϕ_2 of the largest circles inscribed in the cross-section of the trunks and the tangent lines t_1, t_2 of the centroidal curves at points A and B.

- Step 2: Making of types 1 and 3 cuts (Fig. 21) is performed by utilizing sufficiently large size rectangular parallelepipeds (Fig. 32a and b) respectively parallel to t_1 (for the cutting of beam 2) and t_2 (for the cutting of beam 1). Their dimensions are dictated by the input parameters of the connection (E, μ, β_1 or β_2, λ_1 or λ_2 and B_o such as described in section 3.5). The position C of the main plane along the axis AB depends on E, μ and B. The box must follow these rules: the orientation of the box depends on t_1 or t_2; the width of the box depends on λ; the height and length of the box depend on the mesh. Finally, the type 3 cut orientation depends on β_1 or β_2.

- Step 3: Making type 2 cuts (Fig. 21), which corresponds to a pseudo-elliptical shape of cutting volume, results from several geometrical constructions. The parameters used to create this volume are the 3D meshes, t_1 and t_2, β_1 or β_2, λ_1 or λ_2, and C_O. The process is the following: (i) The intersection between the meshes of the two trunks gives the first geometrical limit and only its lower limit i_1 is kept (Fig. 33a), (ii) The segments bisector b_1 and b_2 of tangents t_1 and t_2 are drawn (Fig. 33b). Then, planes p_1 and p_2 are respectively defined by (b_1 and line AC) and (b_2 and line AC). Next, the intersections of planes p_1 and p_2 with the mesh give the second and third initial geometrical limits i_2 and i_3 (Fig. 33c), (iii) Intersections i_1, i_2, and i_3 are assembled to form a closed 3D curve which is projected onto the type 2 cut main plane (Fig. 33e),

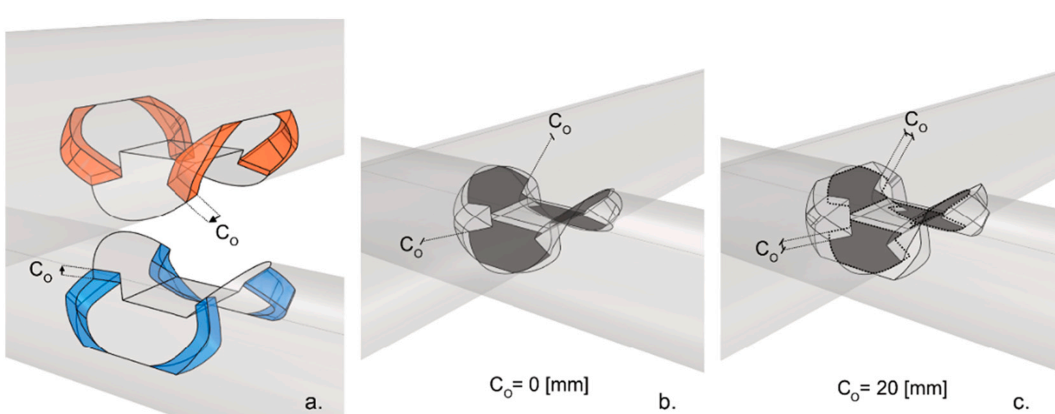

Fig. 30. Physical representation of (a) $C_{O,}$ (b) no cutting offset ($C_O = 0$), and (c) the decrease in contact area between the type 3 cuts when C_o increases.

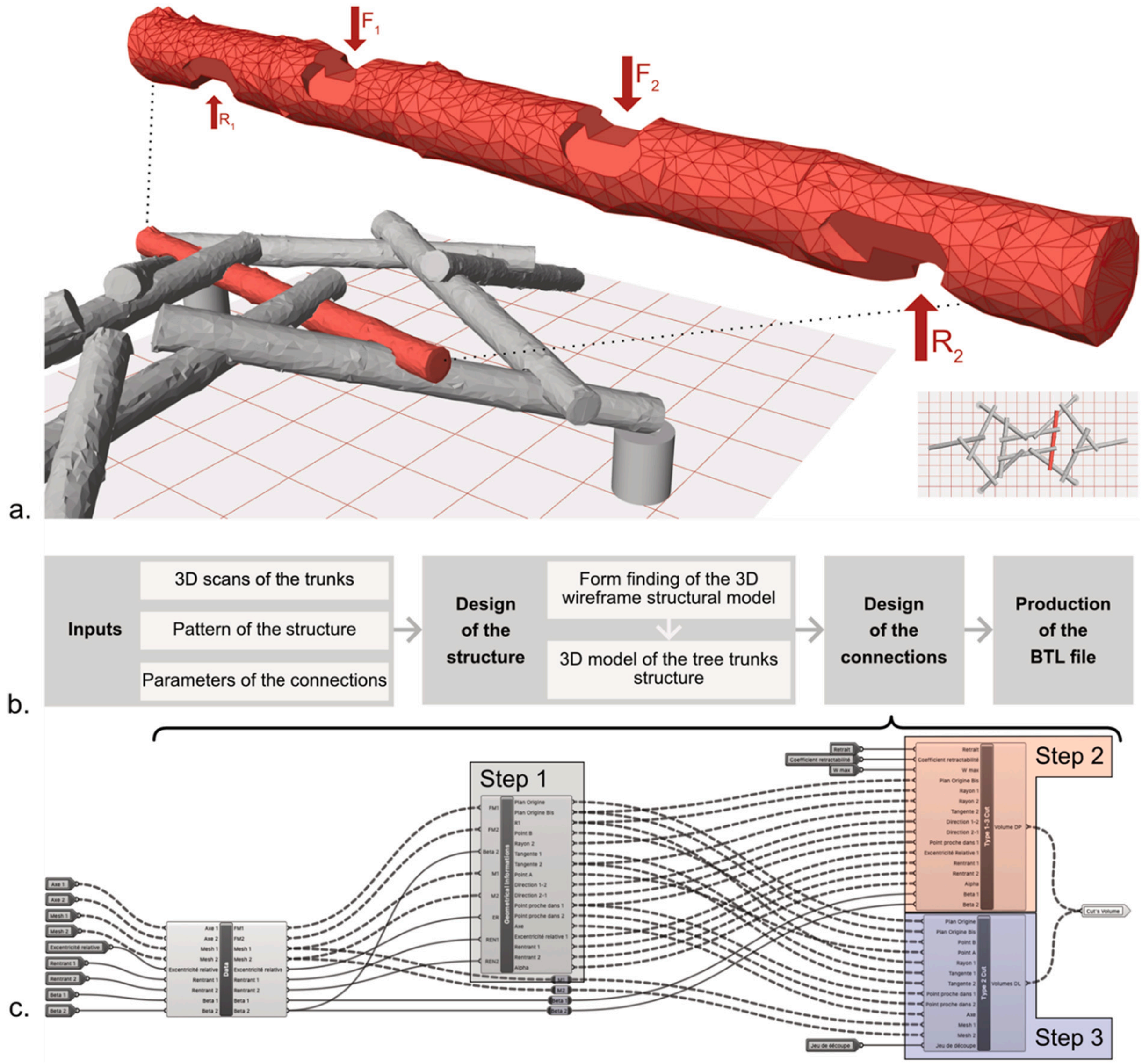

Fig. 31. (a) Typical result of the script developed on Grasshopper, (b) principle of the script, which allows the design of structures composed of tree trunks and their connections, the production of a BTL file that can be used by the robot for the cutting, and (c) the Grasshopper code.

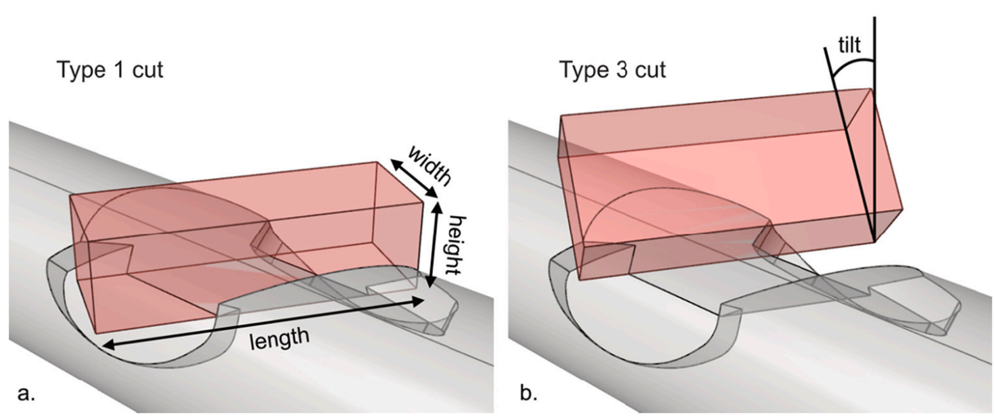

Fig. 32. Examples of cutting volumes of (a) type 1 and (b) type 3 cuts, which are rectangular parallelepipeds with dimensions fixed by the input connector parameters E, μ, B_O, λ, β.

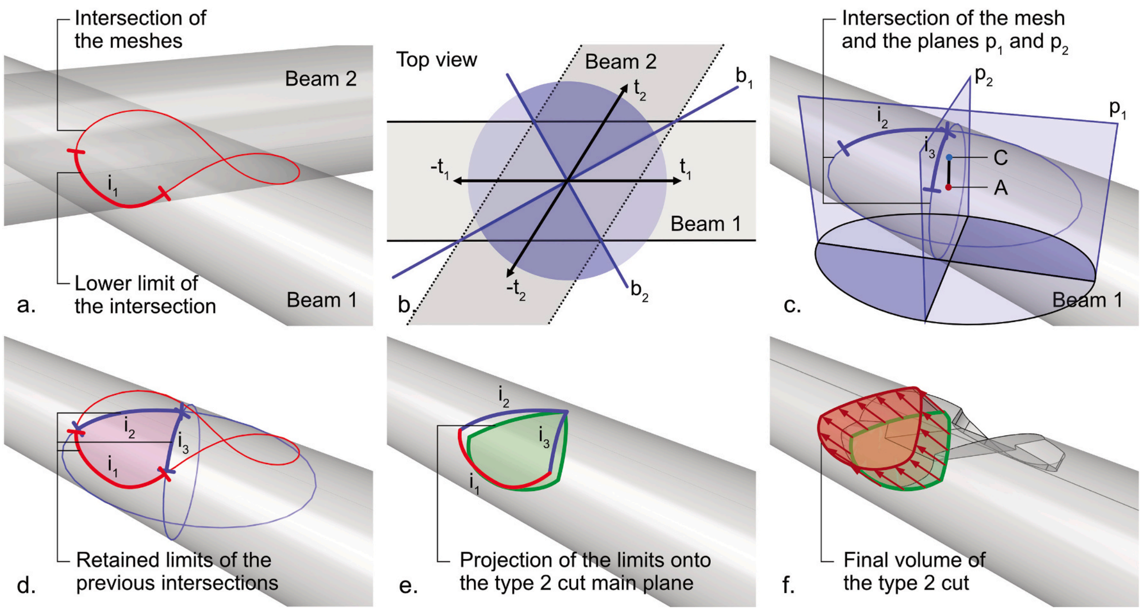

Fig. 33. Flow of geometrical constructions to create the pseudo-elliptical shape of type 2.

(iv) The 2D curve is then expanded by the offset C_0 (Fig. 30). The height of the volume to be cut is based on the mesh of the trunk (Fig. 33f).

3.7. From the parametric design to the robotic arm, via the BTL

The *BTL* format [57] is a free standard developed by a cooperation of machine designers and software developers for data transfer from a design software to wood-cutting machines. The advantage of BTL is that the way cutting is performed does not depend on the designer of the structure, but on the manufacturer of the machine. In other words, the user can be independent of the designer. Therefore, if the cutting tool changes, the BTL file remains the same.

As briefly explained in section 3.6, each notch is made by breaking it down into a series of cutting volumes (Fig. 34). Each of them is hollowed out by the tool in several machining passes. The robotic arm that was used to produce the prototype was equipped with a milling cutter that works perpendicular to the main surfaces of type 1, 2 or 3 cuts, as defined in Fig. 21. Five cutting volumes are required to make a complete notch (Fig. 34). The Grasshopper script described in section 3.6 allows a generated BTL file to be sent to the robot for machining each notch. This file contains the geometrical characteristics, the referencing system, and the type of process (i.e., Lap Joint or Free Contour) of the 5 cutting volumes.

The BTL library currently includes 47 processes developed specifically for woodworking. Only two processes were needed for this project, respectively the “Lap Joint” BTL process for types 1 and 3 cuts, and the “Free Contour” BTL process for the type 2 cut (Fig. 35).

Each process consists of one or more operations called “processidents”. For the “Lap Joint” BTL process, only one processident is needed and it simply consists of digging a rectangular parallelepiped for which the following parameters are provided: (i) the 3 dimensions of the box, (ii) the origin of the local Cartesian coordinate reference system (X,

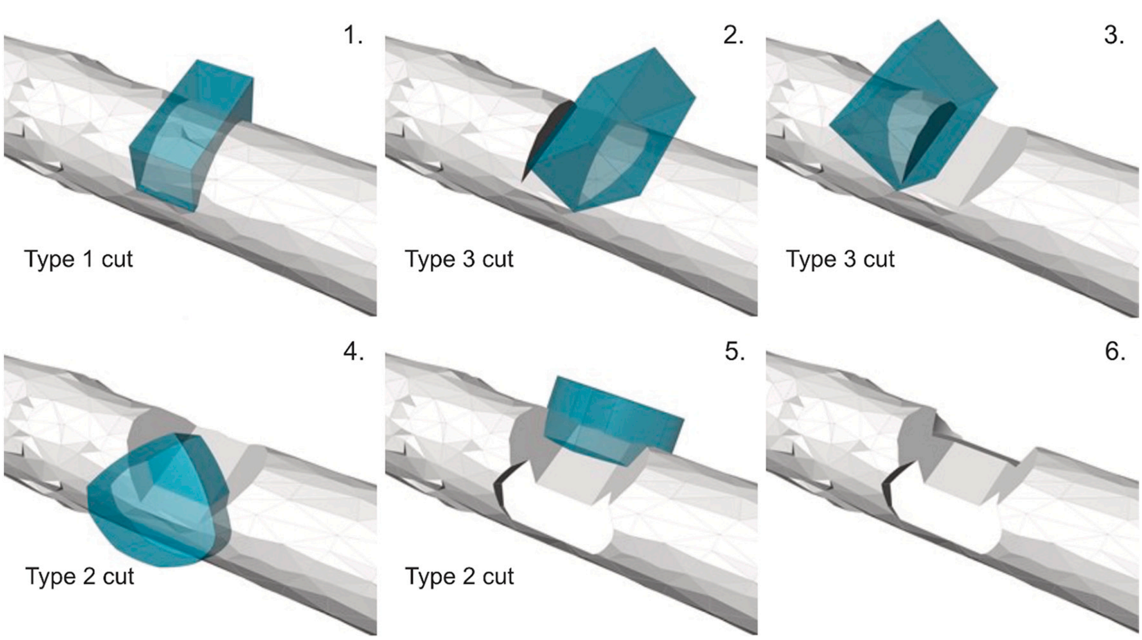

Fig. 34. The 5 cutting volumes required to carve a notch and the completed notch.

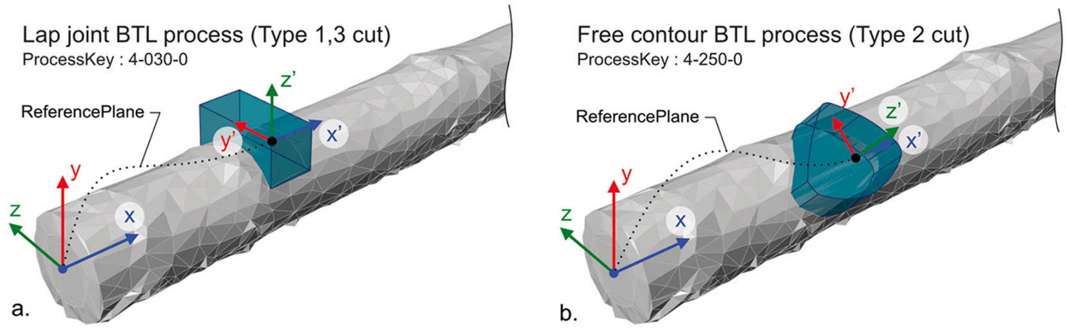

Fig. 35. (a) "Lap Joint" BTL process used for type 1 and type 3 cuts and (b) "Free Contour" BTL process used for type 2 cut.

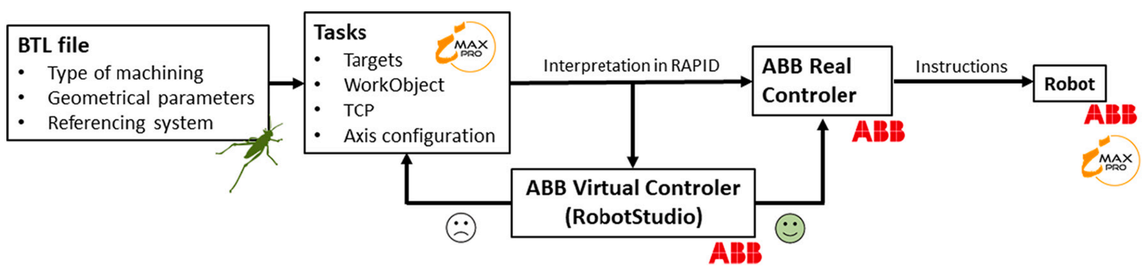

Fig. 36. Translation of a BTL file into robot movement instructions.

Y,Z), and (iii) its orientation. For the "Free Contour" process, several processidents are necessary because the contour of the type 2 cut is a closed curve of complex geometry which must be approximated by a series of circular arcs. Finally, each "processidents" is itself characterized by a maximum of 16 parameters. These parameters correspond to a datum which may, for example, be a dimension, a cutting depth, the starting point of the tool, etc.

The robot used is an ABB IRB 6700 mounted on a track motion system of 40 m length (Fig. 37). It is equipped with a 9.5 kw HSD electric motor and a milling cutter of 40 mm diameter and 160 mm length, and its arm is composed of elements with a total of 6 different rotational axes. The logs to be machined are firmly attached on static trestle. To move the robot tool from one point to another, there are many solutions since the articulated arm is made up of different moving parts. The definition of these movements, with the BTL file as input, is beyond the scope of this article, but Fig. 36 shows the principle of this process. The 5 volumes defined in Fig. 34 represent each a "task" to be performed by the robot. Each "task" is a sequence of operations that drive the movement of the cutting tool, which is defined by the TCP (Tool Central Point), to different points in space called "targets". In addition to this information, the ABB robot controller also needs a "Work Object" (which is the (X, Y, Z) referencing system of the log), and an "Axis Configuration", which globally defines for robot's rotational axes number 1, 4 and 6, in which zone (0° to 360°) a rotation should occur during the movements towards the targets. Targets are created so that the cutting tool traverses the entire cutting volume and depend on the power of the motor, the size of the cutter, and the type of wood (softwood or hardwood). For instance, the layer of removed material in hardwoods is generally finer than in softwoods, which are softer. Finally, tasks are translated from C# programming language to RAPID language so that the ABB controller can give instructions to the robot.

Fig. 37. ABB IRB 6700 robotic arm.

4. Description of the prototype and discussion

A reciprocal structure prototype has been built, shown in Fig. 38. The diameters of the 14 trunks are similar, and the parameters have been set to the following values for each notch: E = 120 mm (average radius of the trunks, the Kangaroo plug-in of *Grasshopper* is used to find the position of all lines that satisfy this eccentricity at each intersection), $\mu = 0.5$, $\beta_1 = \beta_2 = 45^\circ$, $\lambda_1 = \lambda_2 = 0.5$, $B_o = 10$ mm and $C_o = 20$ mm. Figs. 37 and 39 show the 6 degrees of freedom robotic arm that was used to machine the connections. The structure displays excellent rigidity and stability, even with applied point loads. However, two precautionary cables have been added to avoid any slippage due to excess weight as the structure has since been displayed in public and spectators have been known to scale the structure.

The design, prefabrication, and construction of the structure according to the process detailed in this article confirm the validity of this approach and suggests the following comments:

(i) 3D Scanning: Photogrammetry was performed with a basic camera (Fig. 16) and with the Metashape software from Agisoft [56]. The advantage of this solution is the low-cost compared to other scanning technologies such as LiDAR. Furthermore, photogrammetry provides a very high accuracy (1 mm on the shape of any trunk's circumference), which proved to be sufficient for design and machining. The

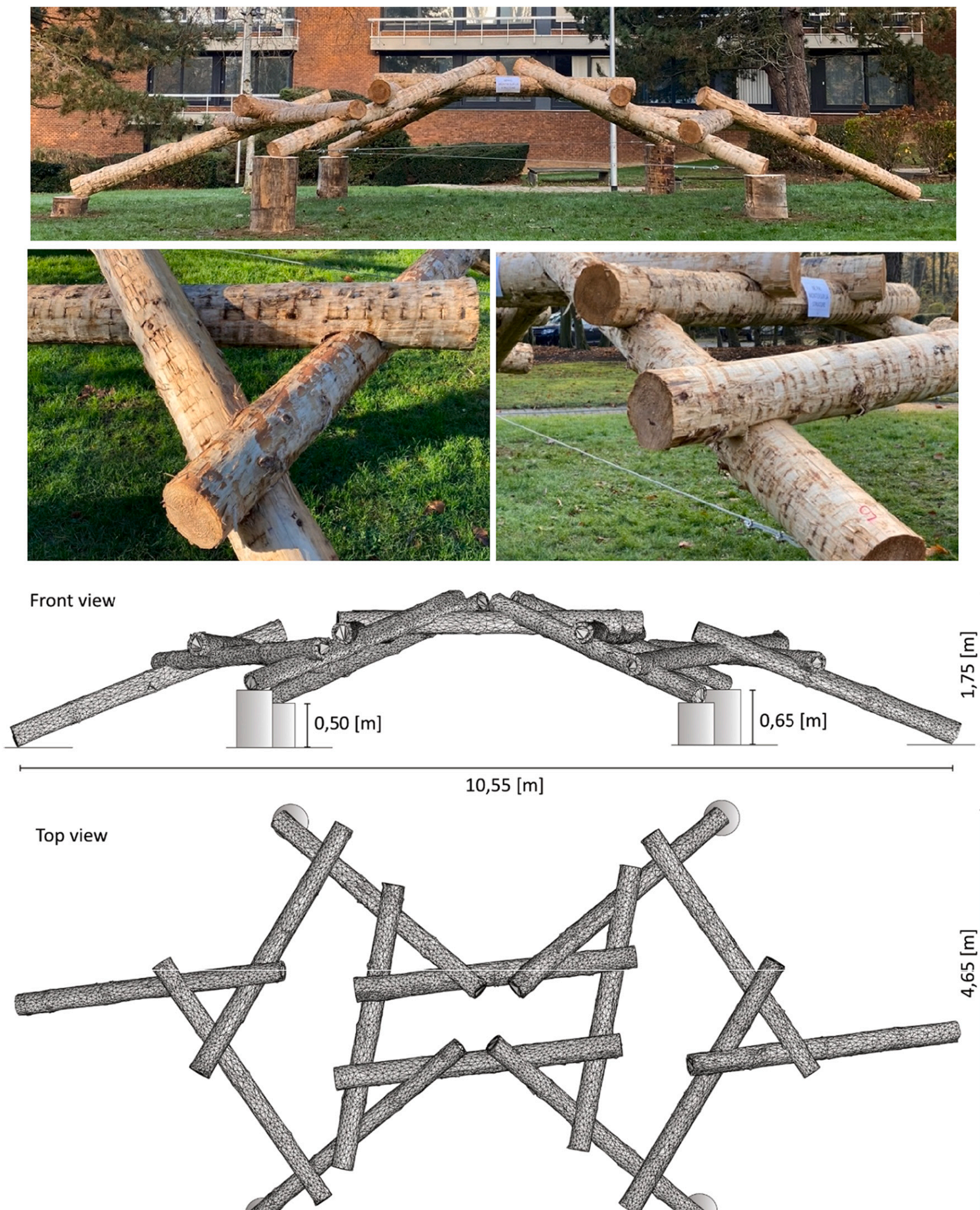

Fig. 38. Reciprocal 3D frame composed of timber logs (from the authors, 2020, videos on: [54,55]).

Fig. 39. Milling of a timber log with a 6 DoF robotic arm (from the authors, 2020, videos on: [54,55]).

disadvantage of photogrammetry made with Metashape is that it requires a manual post processing which is not compatible with an uninterrupted automatic process between design and machining. However, Stathopoulou [58] et al. had developed solutions based on COLMAP [59], OpenMVG+OpenMVS [60] and AliceVision [61] that can automate photogrammetric digitizing. In the case of an industrial process where the optical lenses are sensitive to dust, it is believed that a better solution would be to combine non-destructive mechanical log characterization equipment with laser scanning equipment. This solution would allow the creation of a timely databases that simultaneously includes mechanical and geometrical data of the logs.

(ii) Robotic Arm: A preliminary machining test was performed with a simple manual router mounted on a bench (section 1.2). This test showed that typical tools such as CNC are not adapted to making JJP connections for several reasons, for example, trunks are too long and there are too few degrees of freedom, so consequentially the machining operation is very time consuming (several hours per trunk). Furthermore, positioning the tree trunk in the bench for each new machining reference planes (5 per connection, equating to referencing the tree trunk 20 times in the bench for a beam with 4 connections) can lead to inacceptable inaccuracy. The 6 DoF robotic arm mounted on a sufficiently long track (the one used herein is 40 m long) eliminates these problems. The 9-kW milling cutter's motor, which was used with the robot, completed each connection in about 15 minutes with a measured accuracy better than 2 mm. However, two drawbacks of the robotic arm were raised: (i) Recording the position of the R and S points on the trunk ends with the robotic arm end tool requires an operator and is time-consuming, even if it is done only once per trunk, and (ii) The cutting equipment is long (90 cm), therefore a large amount of free space is needed for the robot around the cutting areas, which may be cumbersome when operating near the trestles supporting the log. In some circumstances, movable trestles or a special support system may be required. Nevertheless, the cutting of the 14 logs in the prototype was done without any loss, all connections conformed with designs, no rectifications were necessary, and no failure was noticed during the cutting.

(iii) Local coordinate reference system (X, Y, Z): The process described in section 3.3 requires the use of a small box attached to the trunks, and the use of paper printouts for the marking of points R and S before Robot Cutting. This is a double disadvantage because on the one hand the small box is fragile when the log is moved, and on the other hand the scoring of R and S requires printing on paper and slows down the process. Another possible process is illustrated in Fig. 40. Before scanning, the points P_1, P_2 and P_3 are marked on the log (with a marker or a simple screw). They are then scanned with the log (the equipment used must therefore allow their detection). Then, these points are added to the mesh and they allow the definition of a local (X, Y, Z) reference system, to which the centroidal axis R-S can then be referenced. The centroidal axis can then be referenced in this local reference frame. Before starting to cut, it is sufficient to point the robot head on the points P_1, P_2 and P_3. This process avoids the above disadvantages (the use of a box and printing on paper before cutting), but it requires more work from an operator during the generation of the mesh.

(iv) BTL Files: The selection of a BTL file produced by the Grasshopper script makes it possible to perform the cuttings with a robotic arm but also with most wood-cutting machines, which is an advantage. The project partner Imax Pro has developed its own algorithms to translate BTL files into robot instructions (Tasks, Targets, WorkObject, TCP and Axes configuration) and this is the second reason why it was decided to produce BTL file from the Grasshopper code.

However, if it is decided that the design tool in Grasshopper is to be used only with a robotic arm, the writing of a BTL file can be avoided, as well as the "translation" imposed by the file and the consequential time loss. This decision requires the code that defines the robot instructions to be directly integrated into the algorithm used in Grasshopper.

(v) On-Site Construction and Connection Behavior: No major difficulties were encountered during the on-site construction of the structure. The JJP connections have ensured a good contact between trunks, even after the timber dried. The precision of the machining and design process were also sufficient. The assembly of the structure was done module by module, each beam placed in a specific order, and the conical shape enabled good guidance and clamping. The 20 mm cutting offset C_O was necessary to enable the insertion the last beam of each module, as a rotation movement of this beam was required.

(vi) Structural Design and Reliability: This article deals mainly with the design aspects of trunk-trunk connections and their machining with robots. However, the structural reliability aspects are a very big challenge in construction with tree trunks. Globally, this includes three distinct aspects. First, it is necessary to develop non-destructive experimental protocols to characterize the individual strength of logs. This may involve testing machines or grading methods similar to those used for squared timber. Secondly, it is necessary to understand how the stress flows at the connections evolve as they are influenced by drying and global movements of the structure. Finally, for reciprocal structures in particular, research is needed to develop calculation methods that account for particular local behaviors of the connections. Of course, the stresses that passed through the connections are influenced by the internal forces in the structure, and vice versa.

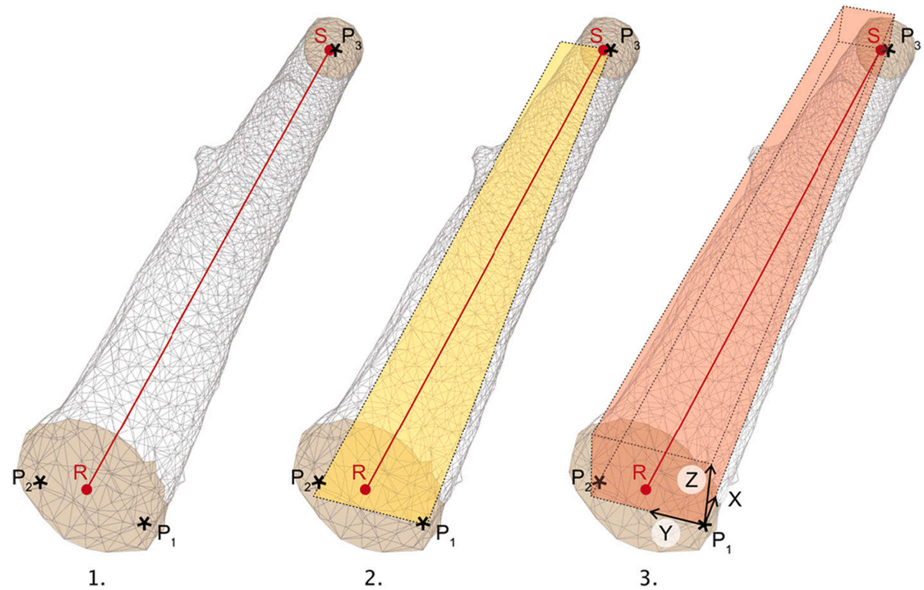

Fig. 40. Alternative for the local coordinate reference system.

5. Conclusion

The use of wood in construction is still very marginal in many countries. There are several reasons for this, but one of the most important reasons is the high cost of the wood-processing industry, which makes timber uncompetitive compared to concrete or steel. Using whole timber in construction therefore makes sense, especially since cutting it into rectangular sections has a negative impact on the mechanical characteristics.

The recent emergence of advanced digitization and robotics means that it is now possible to prepare trunks using this design philosophy to be applied at an industrial level which, only a decade ago, would have been unaffordable and incompatible with modern construction as it required expensive artisanal craftsmen.

The objective of this research was to prove the feasibility of the industrial production of trunk-trunk connections, using a design and manufacturing process based on a semi-direct link between computational design and a robotic arm performing automated cutting. To meet this challenge, these mathematical parameterization of the geometry of wood-wood connections enables good contact, good stacking, easy construction, insensitivity to humidity variations, and good flow of stresses. Next, a code was created in the form of a plug-in for Grasshopper software allowing the design of structures composed of trunks previously scanned in 3D to automatically define the cuts to be made and finally to create a BTL file allowing the delivery of cutting instructions to a robotic arm. A machining bench was also built to demonstrate the relevance of using robotic arms for this type of work. Finally, a full-scale $5\,m \times 10\,m$ prototype made up of 14 trunks was designed, machined, and assembled according to this procedure (Fig. 38). On the principle of "who can do more can do less", this prototype is a so-called reciprocal structure, of which all connections are different. The result is a complete success which now allows the project to move forward by perfecting the methodology to incorporate more automated and efficient design and manufacturing. The research avenues are now the following:

- The development of an efficient and fast 3D scanning tool for trunks (other than photogrammetry which is too time-consuming in post-processing), possibly combined with equipment that allows the mechanical characterization of the trunks.
- The establishment of rules for the selection of the 7 parameters that determine the geometry of the notches according to the respective orientation of the assembled trunks and the value of the forces at the notch. It was shown that the variation of these parameters can have favorable or unfavorable impacts on the quality of interlocking, the capacity to absorb variations in humidity, the transmission of stresses, the inertia of the sections around the joints, and the ease of on-site construction. This is a very broad area that must be investigated to answer the question: for a given connection between two trunks and a given value of the forces to transmit, how can the optimal values of the 7 parameters be found in order to satisfy the perfect transmission of all stresses and forces in the structure?
- In addition to the previous point, further research should incorporate the calculation and design of the overall structure, and not just the connections. This concerns the improvement of the design interface to integrate a global and local calculation tool that allows for an optimal design of the connections (transmission of local contact stresses) and an optimal design of the global structure (transmission of internal forces). Even if this is facilitated by the parametric design, the design of the global structure and the design of each connection are indeed linked and require an iterative algorithm which is insufficiently explored, especially for reciprocal structures.

Regarding the development of a more automated system for defining and recording the local reference system attached to the trunks: This principle has been explained above in reference to the trunks, which is done using a solid box attached to each trunk by means of a metal rod. Before cutting begins, the robot must point at this object and record its position, which requires the intervention of an operator, though this step is likely to slow down the process. To remedy this, the use of a LiDAR attached to the robotic arm and correctly referenced could be a solution. In addition, the storage and handling of logs is likely to damage the solid boxes attached to each log. The use of a LiDAR, referenced to the robot, would be comparable to the 3D mesh used for the design of the cuts and a second 3D mesh made at the time of the cuts could make it possible to know the exact position and orientation of the log on the trestles, and thus avoiding the use of this box.

Declaration of Competing Interest

The authors declare no competing financial or personal interests which could influence the contents of this paper.

Acknowledgments

The authors would like to thank "SPW service public de Wallonie" of Belgium, who funded this research, via the convention ROBOTREE n°8005, "Doctorat en entreprise". The authors would also like to acknowledge that this publication benefits from the support of the Belgian FNRS within the framework of the financing of a FRIA grant. Finally, the authors extend their sincerest gratitude to the Belgian company IMAX Pro and its CEOs Patrick and Cédric Moutschen, who have allowed the use of their robot, their equipment and allowed the authors to benefit from the unique experience of programming robotic arms in the field of timber structures.

References

[1] P. Villoria Sáez, M. Osmani, A diagnosis of construction and demolition waste generation and recovery practice in the European Union, J. Clean. Prod. 241 (2019), https://doi.org/10.1016/j.jclepro.2019.118400.
[2] International Energy Agency, Global Status Report for Buildings and Construction: Towards a Zero-Emission, Efficient and Resilient Buildings and Construction Sector, 2019, ISBN: 978-92-807-3768-4, https://wedocs.unep.org/handle/20.500.11822/30950?show=full, 2019 (accessed January 18, 2022).
[3] A. Bukauskas, P. Mayencourt, P. Shepherd, B. Sharma, C. Mueller, P. Walker, J. Bregulla, Whole timber construction: a state of the art review, Constr. Build. Mater. 213 (2019) 748–769, https://doi.org/10.1016/j.conbuildmat.2019.03.043.
[4] J. Natterer, J.-L. Sandoz, M. Rey, Construction en bois - Matériaux, technologie et dimensionnement, in: Presse Polytechniques et Universitaires Romandes, 2nd ed., 2012. ISBN: 978-2-88074-949-1.
[5] G. Boëthius, A. Zorn, Studier i den nordiska timmerbyggnadskonsten från vikingatiden till 1800-talet: en undersökning utgående från Anders Zorns samlingar i Mora, 1st ed., Fritzes Hovbokhandel, Stockholm, 1927.
[6] Fologram, Instant Mixed Reality Experiences from Rhino and Grasshopper. https://fologram.com/, 2022 accessed October 1, 2021.
[7] A. Pugnale, D. Parigi, P.H. Kirkegaard, M.S. Sassone, The principle of structural reciprocity: history, properties and design issues, in: Full Papers: Taller, Longer, Lighter: Meeting Growing Demand with Limited Resources: IABSE-IASS Symposium 2011, Hemming Group Ltd, 2011, pp. 414–421. ISBN: 978-0-7079-7122-3.
[8] O. Baverel, Nexorades: A Family of Interwoven Space Structures. https://openresearch.surrey.ac.uk/esploro/outputs/doctoral/Nexorades-A-Family-of-Interwoven-Space-Structures/99516811502346#file-0, 2001 accessed December 9, 2021.
[9] D. Parigi, P.H. Kirkegaard, Design and fabrication of free-form reciprocal structures, Nexus Network Journal 16 (2014) 69–87, https://doi.org/10.1007/s00004-014-0177-9.
[10] P. Song, C.-W. Fu, P. Goswami, J. Zheng, N.J. Mitra, D. Cohen-Or, Reciprocal frame structures made easy, ACM Trans. Graph. 32 (2013) 1–13, https://doi.org/10.1145/2461912.2461915.
[11] D. Parigi, P.H. Kirkegaard, Structural behaviour of reciprocal structures, in: Proceedings of IASS Annual Symposia, International Association for Shell and Spatial Structures (IASS), 2013, pp. 1–9. https://www.ingentaconnect.com/content/iass/piass/2013/00002013/00000009/art00009. accessed January 28, 2022.
[12] D. Parigi, A. Pugnale, Three-dimensionality in reciprocal structures: concepts and generative rules, Nexus Network Journal 16 (2014) 151–177, https://doi.org/10.1007/s00004-014-0183-y.
[13] O. Popovic Larsen, Reciprocal Frame Architecture, 1st ed., Routledge, London, 2007. ISBN: 978-0-7506-8263-3.
[14] O. Baverel, H. Nooshin, Y. Kuroiwa, Configuration processing of nexorades using genetic algorithms, J. Int. Assoc. Shell Spatial Struct. 45 (2004) 99–108. https://www.ingentaconnect.com/content/iass/jiass/2004/00000045/00000002/art00005. accessed January 18, 2022.
[15] C. Douthe, O. Baverel, Design of nexorades or reciprocal frame systems with the dynamic relaxation method, Comput. Struct. 87 (2009) 1296–1307, https://doi.org/10.1016/j.compstruc.2009.06.011.
[16] D. Parigi, P.H. Kirkegaard, M. Sassone, Hybrid optimization in the design of reciprocal structures, in: Proceedings of IASS Annual Symposia, International Association for Shell and Spatial Structures (IASS), Seoul, 2012, pp. 1–8, in: https://www.researchgate.net/profile/Mario-Sassone/publication/264890660_Hybrid_optimization_in_the_design_of_reciprocal_structures/links/5421bd630cf238c6ea671efa/Hybrid-optimization-in-the-design-of-reciprocal-structures.pdf. accessed December 9, 2021.
[17] D. Parigi, P.H. Kirkegaard, The Reciprocalizer: an agile design tool for reciprocal structures, Nexus Network Journal 16 (2014) 61–68, https://doi.org/10.1007/s00004-014-0176-x.
[18] U. Thönnissen, A form-finding instrument for reciprocal structures, Nexus Network Journal 16 (2014) 89–107, https://doi.org/10.1007/s00004-014-0172-1.
[19] C. Preisinger, Linking structure and parametric geometry, Archit. Des. 83 (2013) 110–113, https://doi.org/10.1002/ad.1564.
[20] A.A. Apolinarska, Complex Timber Structures from Simple Elements Computational Design of Novel Bar Structures for Robotic Fabrication and Assembly, 2018, https://doi.org/10.3929/ethz-b-000266723.
[21] M. Tamke, M.R. Thomsen, Digital wood craft, in: Joining Languages, Cultures and Visions, 2009, pp. 673–683. https://www.researchgate.net/publication/30875474_Digital_wood_craft. accessed December 9, 2021.
[22] M. Tamke, J. Riiber, H. Jungjohann, M.R. Thomsen, Lamella Flock, in: C. Ceccato, L. Hesselgren, M. Pauly, H. Pottmann, J. Wallner (Eds.), Advances in Architectural Geometry 2010, Springer, Vienna, 2010, pp. 37–48, https://doi.org/10.1007/978-3-7091-0309-8_3.
[23] S. Tuksam, S. Pihlak, Soundwave, Rheological Formation and Bodybuilding, Practice for Architecture, Research and Theory (PART). http://part.archi/#projects, 2021 accessed January 4, 2021.
[24] P.F. Yuan, H. Chai, Reverse Rafter: structural performance simulation based on wood tectonic, in: Proceedings of the Association for Computer-Aided Architectural Design Research in Asia (CAADRIA), 2015, pp. 693–702. http://papers.cumincad.org/data/works/att/caadria2015_145.content.pdf. accessed December 9, 2021.
[25] L. Allner, P. Reinsberg, J. Sato, Interlocking spaces: a structural prototype inspired by Kigumi architecture, in: Proceedings of the International Association for Shell and Spatial Structures (IASS) Symposium, Form and Force, Barcelona, 2019, pp. 1–7. https://www.researchgate.net/profile/Lukas-Allner/publication/337363622_Interlocking_spaces_A_structural_prototype_inspired_by_Kigumi_Architecture/links/5dd40758299bf11ec8625673/Interlocking-spaces-A-structural-prototype-inspired-by-Kigumi-Architecture.pdf. accessed December 9, 2021.
[26] P. Eversmann, F. Gramazio, M. Kohler, Robotic prefabrication of timber structures: towards automated large-scale spatial assembly, Construct. Robot. 1 (2017) 49–60, https://doi.org/10.1007/s41693-017-0006-2.
[27] A.S.-C. Tai, Design for Assembly: A Computational Approach to Construct Interlocking Wooden Frames. http://dspace.mit.edu/bitstream/handle/1721.1/72968/808367239-MIT.pdf;jsessionid=7325A18E084EB192C357515B9DB01F5D?sequence=2, 2012 accessed December 9, 2021.
[28] T. Godthelp, A. Jorissen, A.P.H.W. Habraken, R. Roelofs, The timber reciprocal frame designer: free form design to production, in: C. Lázaro, K.-U. Bletzinger, E. Oñate (Eds.), Form and Force: Proceedings of the International Association for Shell and Spatial Structures (IASS) Symposium, Barcelona, 2019, pp. 2764–2771, in: https://www.researchgate.net/publication/336642227_The_Timber_Reciprocal_Frame_Designer_Free_Form_Design_to_Production. accessed December 9, 2021.
[29] Z. Mollica, Tree Fork Truss: An Architecture of Inherent Forms. https://zacharymolli.ca/assets/download/Mollica-DMThesis-Tree-Fork-Truss-an-Architecture-of-Inherent-Forms.pdf, 2016 accessed December 9, 2021.
[30] H. Yoshida, M. Larsson, T. Igarashi, Upcycling tree branches as architectural elements through collaborative design and fabrication, in: Proceedings of the Thirteenth International Conference on Tangible, Embedded, and Embodied Interaction, ACM, New York, NY, USA, 2019, pp. 589–593, https://doi.org/10.1145/3294109.3295639.
[31] C. Schindler, M. Tamke, A. Tabatabai, M. Bereuter, H. Yoshida, Processing branches: reactivating the performativity of natural wooden form with contemporary information technology, Int. J. Archit. Comput. 12 (2014) 101–115, https://doi.org/10.1260/1475-472X.12.2.101.
[32] V. Monier, J.C. Bignon, G. Duchanois, Use of irregular wood components to design non-standard structures, Adv. Mater. Res. 671–674 (2013) 2337–2343, https://doi.org/10.4028/www.scientific.net/AMR.671-674.2337.
[33] L. Allner, D. Kroehnert, Conceptual joining: branch formations, in: Proceedings of the International Association for Shell and Spatial Structures (IASS) Symposium, Boston, 2018, pp. 1–4. https://conceptual-joining.com/wp-content/uploads/2018/11/IASS18_Paper_Branch-Formations_180520.pdf. accessed December 9, 2021.
[34] T. Pawlofsky, A. Debor, Robotic Fabrication Workshop-Teach the Robot to Use a Chainsaw, Institute for Advanced Architecture of Catalonia (IAAC), 2013. https://www.iaacblog.com/events/robotic-fabrication-the-robotic-sawmill-workshop-tom-pawlofsky/. accessed October 18, 2021.
[35] A.A. Robotic Fabrications, Visiting School, Chainsaw Choreographies, Robotic Fabrications. http://roboticfabrications.aaschool.ac.uk/project/chainsaw-choreographies/, 2016 accessed October 18, 2021.
[36] Bandsawn bands, in: R.L. Johns, N. Foley, W. McGee, M. Ponce de Leon (Eds.), Robotic Fabrication in Architecture, Art and Design 2014, Springer International Publishing, Cham, 2014, pp. 17–32, https://doi.org/10.1007/978-3-319-04663-1_2.
[37] A.A. Robotic Fabrications, Visiting School, Bandsaw Manoeuvres, Robotic Fabrications. http://roboticfabrications.aaschool.ac.uk/project/bandsaw-manoeuvres/, 2017 accessed October 18, 2021.
[38] A.K. Aagaard, N.M. Larsen, Developing a fabrication workflow for irregular sawlogs, Int. J. Archit. Comput. 18 (2020) 270–283, https://doi.org/10.1177/1478077120906736.
[39] L. Lok, S. Zivkovic, B. Havener, X. Ma, A. Mecattaf, Ashen Slices, Hannah Office. https://www.hannah-office.org/work/slice, 2018 accessed October 18, 2021.
[40] A.A. Robotic Fabrications, Visiting School, Circular Saw Tactics, Robotic Fabrications. http://roboticfabrications.aaschool.ac.uk/project/circular-saw-tactics/, 2008 accessed October 18, 2021.
[41] G. Brugnaro, E. Baharlou, L. Vasey, A. Menges, Robotic softness: an adaptive robotic fabrication process for woven structures, in: K. Velikov, S. Ahlquist, M. del Campo (Eds.), Posthuman Frontiers: Data, Designers, and Cognitive Machines:

Proceedings of the Annual Conference of the Association for Computer Aided Design in Architecture (ACADIA), 2016, pp. 154–163. http://cumincad.scix.net/data/works/att/acadia16_154.pdf. accessed January 20, 2022.
[42] G. Brugnaro, S. Hanna, Adaptive robotic carving, in: J. Willmann, P. Block, M. Hutter, K. Bryne, T. Schork (Eds.), Robotic Fabrication in Architecture, Art and Design 2018, Springer International Publishing, Cham, 2019, pp. 336–348, https://doi.org/10.1007/978-3-319-92294-2_26.
[43] N. Argyros, Digital WoodCraft: Design and Fabrication Strategies Based on Natural Wood Characteristics, Institute for Advanced Architecture of Catalonia (IAAC), 2017. http://www.iaacblog.com/programs/digital-woodcraft/. accessed October 18, 2021.
[44] E. Gollob, Branch, Robotic Woodcraft: Towards the Craftsmanship of the Future, 2017, pp. 28–29. http://www.roboticwoodcraft.com/wp-content/uploads/2019/04/RoboticWoodcraft.pdf. (Accessed 18 October 2021).
[45] P. Devadass, F. Dailami, Z. Mollica, M. Self, Robotic fabrication of non-standard material, in: K. Velikov, S. Ahlquist, M. del Campo (Eds.), Posthuman Frontiers: Data, Designers, and Cognitive Machines: Proceedings of the Annual Conference of the Association for Computer Aided Design in Architecture (ACADIA), 2016, pp. 206–213. http://papers.cumincad.org/data/works/att/acadia16_206.pdf. accessed January 20, 2022.
[46] B. Havener, Log Knot. www.bdhavener.com/projects/log-knot#10, 2021 accessed October 18, 2021.
[47] N.M. Larsen, A.K. Aagaard, L.H. Kieffer, Digital workflows for natural wood in construction, in: Proceedings of the Conference of the Association for Computer-Aided Architectural Design Research in Asia (CAADRIA), Bangkok, 2020, pp. 125–134. http://papers.cumincad.org/data/works/att/caadria2020_149.pdf. accessed December 10, 2021.
[48] J.C. Chilton, G. Cowley, J. Westmuckett, B. Gilroy-Scott, Reciprocal frame timber roof at Hill Holt Wood - a case study, in: J. Chilton, I. Mungan (Eds.), From Antiquity to the Present: Proceedings of the International Symposium on Timber Structure, Istanbul, 2009, pp. 383–394, in: https://www.researchgate.net/publication/321315757_Reciprocal_frame_timber_roof_at_Hill_Holt_Wood_-_a_case_study. accessed January 20, 2022.
[49] M. Larsson, H. Yoshida, T. Igarashi, Human-in-the-loop fabrication of 3D surfaces with natural tree branches, in: S.N. Spencer (Ed.), Proceedings of the ACM Symposium on Computational Fabrication, ACM, New York, NY, USA, 2019, pp. 1–12, https://doi.org/10.1145/3328939.3329000.
[50] P. Vestartas, Y. Weinand, Joinery solver for whole timber structures, in: World Conference on Timber Engineering (WCTE), Santiago, 2020. https://infoscience.epfl.ch/record/281960?ln=fr. accessed December 10, 2021.
[51] R. Wolfe, C. Moseley, Small-diameter log evaluation for value-added structural applications, For. Prod. J. 50 (2000) 48–58. https://scholarsbank.uoregon.edu/xmlui/handle/1794/3940?show=full. accessed December 10, 2021.
[52] A. Ranta-Maunus, Round Small-Diameter Timber for Construction: Final Report of Project FAIR CT 95-0091, VTT Publications, Espoo, 1999. No. 383.
[53] UniLog, Products. https://www.unilog.co.nz/, 2021 accessed October 18, 2021.
[54] UCLouvain Génie Civil et Environnemental, Robotic construction under parametric design of whole timber reciprocal structures, in: YouTube, 2020. https://www.youtube.com/watch?v=u9XEXpjEt-c. accessed October 18, 2021.
[55] UCLouvain Génie Civil et Environnemental, Outdoor construction of a reciprocal timber structure (UCLouvain, Belgium), in: YouTube, 2021. https://www.youtube.com/watch?v=bXkFNTCM92A. accessed October 18, 2021.
[56] Agisoft LLC, Agisoft. https://www.agisoft.com/, 2021 accessed October 18, 2021.
[57] Design2machine, BTL. https://design2machine.com/btl/index.html, 2021 accessed October 18, 2021.
[58] E.-K. Stathopoulou, M. Welponer, F. Remondino, Open-source image-based 3D reconstruction pipelines: review, comparison and evaluation, Int. Arch. Photogramm. Remote. Sens. Spat. Inf. Sci. XLII-2/W17 (2019) 331–338, https://doi.org/10.5194/isprs-archives-XLII-2-W17-331-2019.
[59] COLMAP, About. https://colmap.github.io/, 2021 accessed October 18, 2021.
[60] OpenMVS, Open Multiple View Stereovision. https://openmvg.readthedocs.io/en/latest/software/MVS/OpenMVS/, 2021 accessed October 18, 2021.
[61] AliceVision, Photogrammetry. https://alicevision.org/, 2021 accessed October 18, 2021.